HHS Public Access

Author manuscript

Nature. Author manuscript; available in PMC 2019 June 10.

Published in final edited form as:

Nature. 2019 January ; 565(7737): 86–90. doi:10.1038/s41586-018-0793-8.

Identification of pathways required for sustained pain-associated coping behaviors

Tianwen Huang[1,2,†], **Shing-Hong Lin**[1,2,†], **Nathalie M. Malewicz**[3], **Yan Zhang**[1,4,5], **Ying Zhang**[1,6], **Martyn Goulding**[7], **Robert H. LaMotte**[3], and **Qiufu Ma**[1,2,*]

[1]Dana-Farber Cancer Institute, Harvard Medical School, Boston, MA 02115, USA.

[2]Department of Neurobiology, Harvard Medical School, Boston, MA 02115, USA.

[3]Department of Anesthesiology, Yale University School of Medicine, New Haven, Connecticut.

[4]Institute of Acupuncture and Moxibustion, Fudan Institutes of Integrative Medicine; Department of Integrative Medicine and Neurobiology, School of Basic Medical Science, Fudan University, Shanghai, 200032, China.

[5]Cell Electrophysiology Laboratory, Wannan Medical College, Wuhu 241002, China.

[6]Neuroscience Research Institute and Department of Neurobiology, School of Basic Medical Sciences, Key Laboratory for Neuroscience, Ministry of Education/National Health and Family Planning Commission, Peking University, Beijing 100191, China

[7]Molecular Neurobiology Laboratory, The Salk Institute for Biological Studies, 10010 North Torrey Pines Road, La Jolla, CA 92037, USA.

Abstract

Animals and humans display two types of responses to noxious stimuli. The first includes reflexive-defensive responses to prevent or limit injury. A well-known example is the quick withdrawal of one's hand touching a hot object. When the first-line response fails to prevent tissue damage (e.g., a finger is burnt), the resulting pain invokes a second-line coping response, such as licking the injured area to soothe suffering. However, the underlying neural circuits driving these two strings of behaviors remain poorly understood. Here we show that in mice, spinal neurons marked by coexpression of $T\varsigma^{Cre}$ and $Lbx1^{Flpo}$, called $Tac1^{Lbx1}$, drive pain-related coping responses. Ablation of $Tac1^{Lbx1}$ neurons led to loss of persistent licking and conditioned aversion evoked by stimuli that produce sustained pain in humans, including skin pinching and burn injury, without affecting all tested reflexive-defensive reactions. This selective indifference to sustained pain resembles the phenotype seen in humans with lesions of medial thalamic nuclei[1–3].

[*]**Corresponding author.** Qiufu_Ma@dfci.harvard.edu.

[†]Contributed equally to this study

Author contributions: T.H., S.H.L., N.M.M., Yan Z. and Ying Z. performed the experiments and data analyses, Q.M., R.H.L. and M.G supervised the whole study, and T.H., S.H.L., Q.M., R.H.L. and M.G. wrote the manuscript.

Author information. All authors have no conflicting interests. Correspondence and requests for materials should be addressed to Q.M.

Supplementary Information is linked to the online version of the paper at www.nature.com/nature.

Consistently, spinal Tac1 lineage neurons are connected to medial thalamic nuclei, via direct projections and indirect routes through the superior lateral parabrachial nuclei. Furthermore, the anatomical and functional segregation observed at the spinal levels is applied to primary sensory neurons. For example, in response to noxious mechanical stimuli, Mrgprd$^+$ and TRPV1$^+$ nociceptors are required to elicit reflexive and coping responses, respectively. Our studies therefore reveal a fundamental subdivision within the cutaneous somatosensory system. The implications for translational success from preclinical pain studies will be discussed.

The *preprotachykinin 1* (*Tac1*) gene is expressed in spinal neurons responding to noxious stimuli[4]. We used the *Tac1^{Cre}* knock-in mice to characterize spinal *Tac1* lineage neurons. Crossing *Tac1^{Cre}* mice with tdTomato reporter mice revealed that 45.3 ± 3.3% of Tac1^{Cre}-tdTomato$^+$ neurons expressed Tac1 mRNA persistently, and 83.9 ± 2.1% of Tac1 mRNA$^+$ neurons coexpressed tdTomato (Fig. 1a). Most Tac1^{Cre}-tdTomato$^+$ neurons are excitatory (Extended Data Fig. 1a-c). The neurokinin receptor NK1R marks most ascending projection neurons in lamina I[5], 36.6 ± 4.6% of which was labeled by tdTomato (Fig. 1b). To assess ascending projections, we produced intersectional *Tac1^{Cdx2}-tdTomato* mice, in which Flpo is driven from the *Cdx2* gene locus and marks spinal neurons[6]; as such, all tdTomato$^+$ fibers in the brain originate from spinal Tac1 lineage neurons (Extended Data Fig. 1d-e). As a control, we labeled all spinal ascending projection neurons by crossing *Cdx2^{Flpo}* mice with tdTomato reporter mice.

We first examined thalamic nuclei. The ventral posterolateral nucleus (VPL), receiving inputs from the spinal cord, is necessary for sensory discrimination and for unpleasantness evoked by transient, moderate noxious stimuli[7]. The medial thalamic complex (MTC) is required to process unpleasantness evoked by sustained, intense noxious stimuli[1–3]. Tac1^{Cdx2}-tdTomato$^+$ fibers were rarely observed in the VPL (Fig. 1c; Extended Data Fig. 1f), in contrast to the extensive innervation by Cdx2^{Flpo}-tdTomato$^+$ fibers (Extended Data Fig. 1f). The MTC is composed of: i) the medial and lateral habenular nuclei (MHb and LHb), ii) the paraventricular thalamic nucleus (PVT), iii) the medial thalamic nuclei (MTh) composed of the dorsal (MD), central (MC) and ventral (MV) sub-nuclei (Fig. 1d-e). While Cdx2^{Flpo}-derived fibers innervated all these midline nuclei (Extended Data Fig. 1g-h), Tac1^{Cdx2}-tdTomato$^+$ fibers displayed selective innervations in PVT and MTh (Fig. 1d) and the most medial part of LHb (Fig. 1d, arrows). Thus, Tac1^{Cre} marks spinothalamic projection neurons that terminate predominantly within the medial thalamic pathways (Fig. 1f).

The pontine lateral parabrachial nuclei (PBN) serve as another key relay station[8–11], which is organized along the dorsoventral axis. The most ventral external lateral nuclei (PBel), marked by the expression of the calcitonin gene-related peptide (CGRP) and sending neuronal projections to the amygdala, are crucial for rapid defensive reactions to external threats[8]. The dorso-ventral lateral nuclei (PBdvl) are involved with behavioral thermoregulation[10], and the most dorsal superior lateral nuclei (Pbsl) is activated by painful stimuli (see below). We found that Tac1^{Cdx2}-derived tdTomato$^+$ fibers pass through the area lateral to PBel and PBdvl (Fig. 1g-h), and terminate PBsl (Fig. 1g). As a control, Cdx2^{Flpo}-labeled whole spinal neurons innervated all subnuclei (Extended Data Fig. 1i). A selective

synaptic connection between Tac1 neurons and PBsl was confirmed by using the presynaptic bouton marking technique[12] and by optogenetic stimulation of $Tac1^{Cre}$-derived terminals (Extended Data Fig. 2a-d). Furthermore, retrograde labeling confirms that $Tac1^{Cre}$ marks subsets of spinoparabrachial and spinothalamic projection neurons (Extended Data Fig. 3a-b). Notably, PBsl sends projection to the medial thalamic nuclei, but not to the amygdala (Extended Data Fig. 3c-d). Thus, spinal $Tac1^{Cre}$-derived ascending projection neurons are both directly and indirectly connected to medial thalamic nuclei.

To carry out functional studies, we used an intersectional genetic strategy[6,13,14] to express the diphtheria toxin (DTX) receptor DTR in spinal neurons defined by the coexpression of $Tac1^{Cre}$ and $Lbx1^{Flpo}$ (Extended Data Fig. 4a), hereafter referred to as $Tac1^{Lbx1}$. $Tac1^{Lbx1}$ neuron-ablated mice, which additionally carried the tdTomato reporter allele, were generated following DTX injections, resulting in an 88% reduction of spinal $tdTomato^{+}$ neurons (Fig. 2a). Ablation was also observed in trigeminal nuclei, but not dorsal root ganglia (DRG) or other brain regions (Extended Data Fig. 4b). Ablation of $Tac1^{Lbx1}$ neurons did not affect sensorimotor coordination or responses to innocuous tactile stimuli (Extended Data Fig. 4c,d).

We next assessed reflexive-defensive responses to noxious or threatening stimuli. $Tac1^{Lbx1}$ neuron-ablated mice showed subtle, but insignificant changes in withdrawal thresholds to punctate mechanical force evoked by von Frey filaments (Fig. 2b), in contrast to the abolition of such reflexes upon ablation of spinal somatostatin lineage neurons[13]. The ablation mice also displayed normal, or subtle, insignificant changes in, withdrawal latencies to noxious cold (Fig. 2c) or heat (Fig. 2d-e) stimuli. Consistent with their sparse innervations to PBel and PBdvl, $Tac1^{Lbx1}$ neurons were dispensable for defensive reactions mediated by these nuclei. $CGRP^{+}$ neurons in PBel are required to produce jumping when mice are confined to 56 °C hot plate[8], and this escape response remained intact (Fig. 2f). PBel neurons also mediate freezing reactions following fearful events[8]. In an inescapable chamber, both control and $Tac1^{Lbx1}$ neuron-ablated mice produced similar degrees of freezing immediately following repeated electric shocks (Fig. 2g) or after the mice were brought back 30 minutes or two days later (Fig. 2g), indicating normal development of conditioned fear memory to threatening events. Neurons in PBdvl are necessary for behavioral thermoregulation[10], and control and ablation mice displayed indistinguishable temperature preferences (Fig. 2h). All together, $Tac1^{Lbx1}$ neurons are largely dispensable for reflexive-defensive responses to external threats.

We next assessed behavioral responses evoked by prolonged noxious stimuli that should produce tissue damage and pain perception. We first placed individual mice in a hot or cold plate chamber until the cut-off time. On the 46–47 °C hot plate, wild type mice showed temporally segregated behaviors, with paw lifting/flinching preceding paw licking, and the emergence of licking correlated with c-Fos induction in $Tac1^{Cre}$-$tdTomato^{+}$ neurons (Extended Data Fig. 4e-f). Licking likely represents a form of coping behavior serving to soothe pain-invoked suffering, potentially via activation of low threshold mechanoreceptors that provide a gate control of pain[15,16]. $Tac1^{Lbx1}$ neuron-ablated mice showed an abolition of licking responses evoked by noxious thermal stimulation (Fig. 3a-b). The transient receptor potential channel TRPA1 serves as a sensor of tissue injury[17,18]. Intraplantar

injection of mustard oil, a TRPA1 agonist that in humans produces sustained burning pain[19], resulted in licking responses lasting for 15 minutes in control mice, but virtually none in ablation mice (Fig. 3c). We further developed a hindpaw burn injury pain model, which led to persistent licking throughout the 30-minute post-injury period. Once again, this coping response was greatly reduced in $Tac1^{Lbx1}$ neuron-ablated mice (Fig. 3d). Top-down execution of the licking motor behavior *per se* is, however, not impaired, since the ablation mice retained licking responses to intraplantar capsaicin injection; this finding also suggests the existence of $Tac1^{Lbx1}$ neuron-independent pain pathways (Extended Data Fig. 5).

Next we assessed mechanical pain-invoked perceptions and behaviors. Human psychophysical studies showed that skin pinching with an alligator clip evoked a pain perception with pricking-aching-burning components (Extended Data Fig. 6). Interestingly, both continuous pain ratings in humans and licking in mice reached peak within 10–15 seconds, and maintained at peak levels throughout the remaining one-minute period (Fig. 3e). This persistent licking was virtually abolished in $Tac1^{Lbx1}$ neuron-ablated mice (Fig. 3f; Supplementary Videos 1 and 2). In accordance with this finding, pinch-induced c-Fos expression in the dorsal spinal cord and in two brain nuclei innervated by $Tac1^{Cre}$-derived spinal neurons (viz., PBsl and MTC) was greatly attenuated in ablation mice (Extended Data Fig. 7a-d). This selective loss of sustained, affective pain-indicative coping responses mimics the phenotypes seen in humans with lesions in medial thalamic nuclei[1,2], consistent with direct and indirect connection of spinal Tac1 neurons to these nuclei (Fig. 1).

Differential impact of $Tac1^{Lbx1}$ neuron ablation on distinct strings of behaviors was also apparent for stimuli that produce itch-related scratching. Short-lasting scratching evoked by external tactile stimulation may evolve as a defensive reaction to remove bugs or parasites touching the skin[14]. This defensive behavior, evoked by light punctate stimulation onto the skin behind an ear, was preserved in $Tac1^{Lbx1}$ neuron-ablated mice (Extended Data Fig. 7e). In contrast, persistent scratching caused by inescapable intradermal exposure to pruritic compounds was greatly attenuated in ablation mice (Extended Data Fig. 7f), consistent with extensive innervations of spinal Tac1 neurons to PBsl, which was part of the PB processing chemical itch[11]. Thus, regardless of thermal, mechanical or pruritic stimuli tested so far, $Tac1^{Lbx1}$-derived spinal neurons, which should include both projection neurons and interneurons, are dispensable for reflexive-defensive reactions to external threats, but necessary for coping behaviors directed toward sustained, inescapable injury or irritation of the skin.

Since sustained skin pinching produces pain and discomfort (Extended Data Fig. 6), we postulated that it should produce strong negative teaching signals allowing animals to learn to avoid such stimuli. To test this, we developed a pinch-evoked conditioned place aversion (CPA) assay (Extended Data Fig. 8a, b). After four training sessions, both male and female control littermates showed an aversion to the pinch-paired compartment, and as a control, sham handling did not produce CPA (Fig. 3g, Extended Data Fig. 8c). $Tac1^{Lbx1}$ neuron-ablated mice were largely insensitive to this conditioning (Fig. 3g, Extended Data Fig. 8d). For a further comparison, repeated radiant heat stimuli, which elicited escapable withdrawal responses (Fig. 2d), failed to produce CPA in either control or ablation mice (Fig. 3g). Thus,

Tac1^{Lbx1} neurons are necessary for conditioned learning and/or memory evoked by stimuli producing sustained pain.

We next assessed if activation of Tac1^{Cre}-derived ascending terminals was sufficient to produce CPA. We used virus approaches to drive the expression of ChR2-EYFP (channelrhodopsin-2 fused with yellow fluorescent protein) or the control RFP (red fluorescent protein) in adult lumbar Tac1^{Cre}-derived spinal neurons (Fig. 3h; Extended Data Fig. 9a). Using a two-chamber avoidance assay[9], we found that optogenetic activation of Tac1^{Cre}-derived terminals in the PBsl area induced robust avoidance during training sessions and post-training aversion to the stimulated chamber (Fig. 3h, Extended Fig. 9b-c). Stimulation of central terminals in the medial thalamic region produced similar consequences (Extended Data Fig. 9d-f). Thus, activation of Tac1^{Cre}-derived ascending projection neurons produced sufficient negative teaching signals and aversive memory for CPA manifestation.

We next asked if the anatomical and functional segregation observed at the spinal level is applied to primary sensory neurons, by re-visiting two largely non-overlapped nociceptors marked by the expression of Mrgprd and TRPV1[20]. Anatomically, Mrgprd$^+$ and TRPV1$^+$ neurons innervate the skin epidermis[21] and the whole body[22,23], respectively (Fig. 4a). We used *Mrgprd^{DTR}* mice to ablate adult Mrgprd$^+$ neurons, and intrathecal capsaicin injection to ablate the central terminals of TRPV1$^+$ nociceptors (Fig. 4b), as reported previously[20]. Ablation of Mrgprd$^+$ neurons caused an increase in withdrawal thresholds to the von Frey filament stimulation, without changing pinch-evoked licking responses (Fig. 4c), mimicking phenotypes seen in mice with ablation of spinal VGLUT3 lineage neurons[24]. Conversely, ablation of TRPV1$^+$ terminals did not affect withdrawal responses to von Frey filament and noxious cold stimulations, but caused a reduction in licking evoked by skin pinching, cold or hot plate stimulation, or skin burn injury (Fig. 4c; Extended Data Fig. 10a-c), thereby mimicking phenotypes seen in Tac1^{Lbx1} neuron-ablated mice. We then found that pinch-induced c-Fos expression in Tac1^{Cre}-tdTomato$^+$ neurons was reduced upon ablation of TRPV1$^+$ terminals, suggesting a functional connection between these neurons (Extended Data Fig. 10d). It should be noted that although TRPV1$^+$ nociceptors are required for both reflexes and licking evoked by noxious heat, separate subsets might involve with these behaviors (Extended Data Fig. 10). Thus, using coping rather than reflex assays, we have reversed a previously held conclusion[20]: TRPV1$^+$, rather than Mrgprd$^+$ nociceptors are required to drive acute sustained mechanical pain. Our findings could explain a long-standing puzzle in humans: in response to skin pinching, first-wave firing by polymodal nociceptors, likely including Mrgprd$^+$-like neurons, does not correlate with pain ratings[25]; pain ratings instead correlate with the firing of capsaicin-sensitive silent nociceptors that gain mechanical sensitivity during prolonged noxious stimuli[26,27].

In summary (Fig. 4d), our studies reveal a fundamental subdivision within the cutaneous somatosensory system, with separate pathways driving reflexive-defensive versus coping responses, two strings of behaviors that reflect exteroception (viz., external threats) versus interoception (viz., internal body injury), respectively. Notably, the concurrent loss of licking or scratching evoked by inescapable noxious mechanical, heat, cold and pruritic stimuli suggests that spinal Tac1^{Lbx1} neurons as a whole population have a general role in driving

the affective component of sustained pain or itch in a sensory modality-independent manner. Our findings challenge the validity of using reflexive-defensive responses to measure sustained pain, and their wide usage for decades may contribute to poor translation from preclinical studies[28,29], echoing a similar argument by LeDoux for the anxiety field[30].

Methods

Mice.

Animal experiments were performed with protocols approved by the Institutional Animal Care and Use Committee. Mice were housed at room temperature with a 12-h/12-h light/dark cycle and had libitum access to standard lab mouse pellet food and water. *Preprotachykinin 1-IRES2-Cre* knock-in mice (*Tac1*^{Cre}, #021877), *Rosa26*$^{LSL\text{-}tdTomato}$ reporter mice ("*Ai14*", #007908), *Rosa26*$^{LSL\text{-}FSF\text{-}tdTomato}$ reporter mice ("*Ai65*", #021875), and *Rosa26*$^{LSL\text{-}FSF\text{-}CatCh}$ mice ("*Ai80*", #025109) were acquired from Jackson Laboratory (JAX). The Flpo-dependent reporter strain was generated by crossing *Ai65* with *Meox2*^{Cre} deleter strain (JAX, #003755) to remove the *loxP*-flanked STOP cassette ("*LSL*"). The intersectional GFP reporter line *Rosa26*$^{FSF\text{-}loxP\text{-}mCherry\text{-}STOP\text{-}loxP\text{-}EGFP}$ (*RC::FrePe*) was provided by Dr. Dymecki[31]. The generation of *Lbx1*^{Flpo}, *Tau*$^{ds\text{-}DTR}$ and *Cdx2*^{Flpo} mice had been described previously[6,13,32]. *Mrgprd*^{DTR} mice, produced in Dr. David J. Anderson lab[20], were provided by Dr. Mark Hoon.

To generate Tac1^{Lbx1} neuron-ablated mice, 6–10 week old male and female *Tac1*$^{Cre/+}$;*Lbx1*$^{Flpo/+}$;*Tau*$^{ds\text{-}DTR/+}$ mice (additionally carrying *Ai14* reporter allele) were injected intraperitoneally (i.p.) with diphtheria toxin (DTX, 50 μg/kg, Sigma-Aldrich, D0564) twice with 72-hour interval. Behavioral and histochemical analyses were performed 30 days later. Littermates lacking either *Lbx1*^{Flpo} or *Tac1*^{Cre} allele but receiving the same DTX injections were used as control. To ablate Mrgprd^{+} neurons, we performed 5 consecutive daily DTX i.p. injections (20 μg/kg) in *Mrgprd*$^{DTR/+}$ mice and their control littermates.

To characterize Tac1^{Cre}-tdTomato^{+} neurons, we analyzed 18–25 lumbar spinal cord sections from three P30 *Tac1*^{Cre}*; Ai14* mice. To test ablation efficiency, we used 4 pairs of 12 weeks old control and ablation mice. For each behavioral analysis, 6–15 pairs of 10 to 14-week old ablation and control mice, including males and females, were used. Animals were randomly assigned into treatment groups and behavior responses were measured in a blinded manner.

Intrathecal (i.t) capsaicin injection.

8 weeks old 129 wild type mice (JAX, #002448) were anesthetized with 2% isoflurane and injected with 5 μl capsaicin (i.t., 10 μg, Sigma, M2028) or vehicle (10% ethanol and 10% Tween-80 in saline) at the pelvic girdle level. Behavioral tests were performed 7 to 14 days later.

Fluorogold retrograde labeling.

Adult *Tac1*^{Cre}*-tdTomato* mice were anesthetized with i.p. injection of ketamine/xylazine mixture (87.5/12.5 mg per kg). The head was mounted on the stereotaxic frame (Stoelting).

After surgical exposure of the brain surface, 0.3 μl Fluorogold (Fluorochrome, 2% in sterilized water) was injected into the medial thalamic complex (AP: −1.58 mm; ML: 0 mm; DV: −2.5 mm from brain surface) or lateral parabrachial nucleus (AP: −5.1 mm; ML: −1.3 mm; DV: −2.3 mm from brain surface) via a glass micropipette driven by picospritzer. The animals recovered for 7 days before tissue collection.

Electrophysiological recording.

The brains from 6 weeks old *Tac1*^{Cdx2}-*CatCh* mice, whose generation was described in Extended Data Fig. 2, were freshly dissected and coronally sectioned by Leica-VT1000s vibratome at 400 μm thickness in ice-cold modified artificial cerebrospinal fluid (ACSF) reported previously[24]. Brain slices covering parabrachial nuclei (Bregma −5.20 ± 0.20 mm) were incubated in the recording solution as reported previously[24], for at least 1 hour in room temperature. The brain slice was then transferred into a recording chamber and perfused with oxygenated recording solution as reported previously[24]. The location of PBsl and PBel subnuclei were visually identified under bright field and neurons within the target area were randomly picked and patched extracellularly. The 473nm blue light (0.2 Hz, 20 ms wave width, 10mW) was delivered and the responses were recorded at voltage clamp mode (holding membrane potential at −70 mV) and then at current clamp mode.

Intraspinal AAV viral injection.

The Cre-dependent AAV plasmids phSyn1(S)-FLEX-tdTomato-T2A-SypEGFP-WPRE (#51509) and pAAV-EF1α-DIO-hChR2(H134R)-EYFP-WPRE-HGHpA (AAV-DIO-ChR2, #20298) were acquired from Addgene. The hChR2(H134R)-EYFP fragment was replaced by a RFP cassette to generate plasmid pAAV-EF1α-DIO-RFP-WPRE-HGHpA. These plasmids were then packed in the AAV2/8 serotype in Boston Children's Hospital Viral Core at the titers of 1.06E+15 gc/ml, 5.776E+13 gc/ml, and 4.520E+13 gc/ml, respectively. Adult *Tac1*^{Cre} mice were anesthetized by ketamine/xylazine (see above). Lumbar vertebrae were exposed by laminectomy, and AAVs were infused bilaterally into the lateral border of the gray/white matters of the dorsal horn (3 spots for each side, 0.3 μl/spot), at 300 μm from dorsal surface and with 500 μm interspaces. AAVs were delivered by picospritzer via a glass micropipette. The tip was left in the spinal cord for additional 5 minutes before pulled out. After 3-week recovery, mice were used for optogentic studies (see below) or euthanized for histochemical studies.

Stereotaxic optic fiber implantation.

Under anesthetic conditions the mouse head was mounted on the stereotaxic frame as described above. After brain exposure, an optical fiber (material: Ceram; ferrule O.D: 2.5 mm; fiber core: 400 μm; fiber length: 3.0 mm; ThorLabs) was implanted above PBsl (AP: −5.1 mm; ML: −1.3 mm; DV: −2.3 mm from brain surface), or above the medial thalamic complex (AP: −1.58 mm; ML: 0 mm; DV: −2.5 mm from brain surface). The optic fibers were secured by mounting dental cement on the skull. After 1-week recovery, mice were subjected to behavioral studies or c-Fos induction analyses following optogentic stimulations.

Histology.

Mice were euthanized by CO_2 and then perfused with 4% paraformaldehyde prepared in 1 × PBS, pH7.4. The brain, spinal cord and lumbar DRGs were dissected and processed (25 μm thickness for brain sections, 16 μm for spinal cord and DRG sections) for immunofluorescent staining as described previously[13,24].

To investigate pinch- or blue light-induced c-Fos expression, mice were euthanized 120 minutes after stimulation, and post-fixed brains were sectioned with vibratome at 75 μm thickness. Free-floating sections were performed to detect c-Fos$^+$ cells using the VECTASTAIN Elite ABC Kits (Vector Labs, #PK-6101). For co-staining of ChR2-EYFP with CGRP in PBN, after visualizing ChR2-EYFP$^+$ fibers by the Nickel-DAB solution (dark blue), brain slices were incubated with mouse anti-CGRP for 16 hours at 4°C. Sections were then washed with PBST and incubated with HRP-conjugated goat-anti-mouse secondary antibody for 1 hour at RT. CGRP$^+$ signals (brown color) was visualized with DAB in PBS containing 0.03% H_2O_2. Color images were taken by Leica DMLB microscope.

Primary antibodies: rabbit anti-c-Fos (Millipore, ABE457, 1:1000 for immunofluorescent and 1:5000 for DAB staining), rabbit anti-CGRP (Millipore, PC205, 1:1000), mouse anti-CGRP (Sigma, C7113, 1:1000), rabbit anti-GFP (Invitrogen, A11122, 1:1000), rabbit anti-NK1R (Sigma, S8305, 1:1000), rabbit anti-TRPV1 (Alomone Labs, ACC-030, 1:1000). Secondary antibodies: goat anti-rabbit IgG-Alexa 488 (Invitrogen, A11034, 1:500), biotinylated goat-anti-rabbit IgG (Vector Labs, BA-1000, 1:1000), HRP-conjugated goat-anti-mouse IgG (Bio-Rad, 1706516, 1:1000).

In situ hybridization (ISH) combined with immunohistochemistry procedures were performed as described previously[33,34].

Behavioral tests.

For all behavioral tests, animals were habituated for 30 min per day consecutively for 3 days before testing. The experimenters were blinded to genotypes and treatments. The subsequent statistical analyses include all data points, no methods were used to pre-determine the sample sizes. Littermates were used as control.

The following behavioral assays were performed as described previously[6,13,24,35–37]: rotarod, light touch (brush), radiant heat (Hargreave's), cold plantar test (dry ice), hot plate, cold plate, von Frey filament test, two-plate temperature preference test, and touch- or chemical compound-induced scratching test. In hot/cold plate tests, only hindpaw lifting/flinching and licking were analyzed. Different cutoffs were set for each hot or cold plate test: 4 min for 46 °C, 3 min for 47 °C, 1 min for 50 °C, 30 s for 56 °C, and 5 min for 0 °C. For c-Fos induction by different hot plate temperatures (see below), the cutoff was 3 min for both 46 °C and 50 °C.

For touch-evoked scratching behavior, each mouse was lightly anaesthetized by 2% isoflurane and the hairs behind the ear were shaved. After recovering from anesthesia, animals were placed into the test chamber for a 1 hour-habituation. A von Frey filament

(0.07 g) was used to poke the shaved skin area. The incidence of scratching responses in ten trials was determined for each mouse.

Mustard oil (MO) test was performed by intraplantar injection to one hindpaw (Sigma, 377430–5G, 0.15% in saline, 20 μl/animal). Capsaicin test was performed similarly (Sigma, M2028, either 3 μg or 0.03 μg/animal in 10 μl saline containing 10% ethanol and 10% Tween-80). Animals were video recorded for 15 min (MO) or 5 min (capsaicin) to determine licking durations.

Skin burn injury pain test was performed by immersing the distal half of mouse right hindpaw into 60 °C water bath for 30 s under deep anesthesia condition (3% isoflurane inhalation via a precise vaporizer). Each mouse was placed in an observation chamber (7.5 cm L × 7.5 cm W × 7.5 cm H) to recover from anesthesia (took ~5 minutes), and then video recorded for 30 min to determine licking durations. The mice were euthanized immediately since pilot studies showed that necrosis would have developed within 3 days.

For pinch assay, each mouse was confined in a plexiglass chamber (10 cm L × 10 cm W × 12 cm H) placed onto a glass, allowing video recording from the bottom. An alligator clip (Amazon, “Generic Micro Steel Toothless Alligator Test Clips 5AMP”) producing 340g force (see below for force calculation) was applied to the ventral skin surface between the footpad and the heel (Extended Data Fig. 8a). The animal was placed back into the chamber and video recorded for 60 s to determine licking duration.

To measure pinch-evoked negative valence, we developed a conditioned place aversion (CPA) assay. The CPA chamber (30 cm L × 30 cm W × 20 cm H) includes compartments “a” and “b”. In “a” compartment, the wall was black plexiglass, and the floor was made up by a set of stainless steel bars (3 mm in diameter, 1 cm interval between bars); in “b” compartment, the wall was decorated by black/white vertical strips with 1 cm width, and the floor was made up by a piece of stainless steel with holes of 8 mm diameter. The procedure includes three sessions, baseline measurement (Day 1), training (Day 2 – 5), and test (Day 6). For every training day, in the morning, each mouse was confined in compartment “a”, and was grabbed for three times with 5 min interval, without pinch stimulation; in the afternoon, each mouse was confined to compartment “b”, and received 3 trials of hindpaw skin pinching: 1 min for each trial with 4 min interval. For baseline and test day measurement, each mouse had free access to both compartments for 15 min, and time spent in “b” was determined. Another set of wild type littermates was used as sham control, receiving grabbing without pinching in both chambers. For radiant heat-evoked CPA measurement, each training session contained 15 trials of radiant heat stimulation to the hindpaw. In our radiant heat test, the average withdrawal latency for wild type mice was ~12 s; as thus the total stimulation time (12 × 15 = 180 s) matched the total duration of skin pinching for the pinch-evoked CPA assay.

In foot shock test, animals were habituated for 3 days. On test day, each mouse got free exploration in a customized foot shock chamber for 5 min, followed by three consecutive electric foot shocks (0.5 mA, 2 s duration, 3 min interval). The mice were returned to their home cage. 30 min and 48 hours later, we then performed re-call tests by placing mice back

to the shock-paired chamber. The mice were video-recorded, and freezing episodes were defined as complete absence of movement except for animal breathing, which was automatically judged and analyzed by ANY-maze behavior tracking software according to its default settings (Freezing "on" threshold score = 30, Freezing "off" threshold score = 40, minimum freeze duration = 250 ms). The electric shock was delivered by a stimulator (Model #3800, A-M Systems) and an isolator (Model #3820, A-M Systems).

Two-trial avoidance task with optogenetic activation.

Tac1^{Cre}-ChR2 and *Tac1*^{Cre}-RFP mice were used for PBN-optogenetic activation test. A 4-day training paradigm was performed. The apparatus was similar as that used for pinch-induced CPA, with small modification of texture cues: in "a" compartment, the floor was composed of thinner stainless steel bars (1 mm in diameter, 2 mm interval); in "b" compartment, the floor was made up by a piece of wire mesh with grid of 5 mm × 5 mm. Mice had no initial preference for one of two compartments ("a": 436 ± 26 s vs. "b": 464 ± 26 s, n = 9, two sided paired t-test, $P = 0.604$). On Day 1 and day 4, each mouse was allowed to freely explore in the chamber for 15 minutes. Avoidance training sessions (15 min / trial) were performed on Day 2 (Trial - 1) and Day 3 (Trial - 2). When a mouse walked into and stayed in the paired compartment, the 473 nm blue light (30 Hz, 20 ms pulse width, 10 mW, Opto Engine LLC., Laser Model #PSU-III-LED) was delivered to PBN. Laser was off immediately after the mouse left the paired compartment with its four paws. Mice were video recorded and the time spent in the blue light-paired compartment were calculated. The aversion score was calculated by the reduction of time spent in blue light-paired compartment on Day 4 ("t_2") in comparison with Day 1 ("t_1"), or during the trials.

The *Tac1*^{Cdx2}-*CatCh* and control *Tac1*^{Cdx2}-*GFP* mice were used for optogenetic activation of spinal Tac1^{Cre}-derived terminals in the medial thalamic complex. The same paradigm was performed as described above.

c-Fos induction.

To study heat-evoked c-Fos expression, each mouse was placed on 46 °C or 50 °C hot plate for 3 min. To study the pinch-evoked c-Fos expression in the spinal cord, each mouse was first habituated as it did for the pinch behavioral assay (see "Behavior tests"), and 3 trials of 30 s-hind paw skin pinch was applied with 5 min interval.

To study pinch-evoked c-Fos expression in the brain, we had to minimize the background c-Fos expression. To do this, each mouse was housed alone for three days; animals were subjected to gentle grabbing and holding for 10 s for five times every day in their home cages, and the mouse was also placed into a new empty cage individually for 120 min, before returning to the original home cage. On the test day, each mouse was habituated in the aforementioned empty cage for 30 min, and only one single-trial of 180 s skin pinch was applied to left hind paw.

To study blue light-induced c-Fos expression, each mouse expressing ChR2, RFP, CatCh or GFP was habituated in the CPA apparatus for 4 hours, and then received a 15-min (20 s light-on with 40 s light-off interval) blue light stimulation (30 Hz, 20 ms pulse width, 10 mW).

After pinch or blue light stimulation, animals were kept in the same apparatus for 120 min, and spinal and brain tissues were then processed as described above.

Skin pinch study in human subjects.

The protocols for the recruitment and testing of human subjects were approved by the Yale University Human Investigative Committee. 12 healthy women and 13 healthy men gave their written, informed consent to participate in the study. The aim was to measure the time course, magnitude and quality of pain sensation reported by humans when pinched by the alligator clip used in similar fashion to test pain-like behavior in mice. Firstly, the force applied by the clip was measured in the Yale Medical School machine shop (Anthony DeSimone): With the bottom jaw of the clip fixed in a milling machine, a wire attached at one end to the upper jaw (strengthened to prevent bending) and the other end of the wire attached to a digital force measuring device, the minimal lifting force required to achieve an opening or gap of 0.1 mm between the jaws was 340 gram (approximately the width of the skin fold between the jaws when the clip was applied to the hind paw skin of a mouse). A force of 440 gram was required for an opening-gap of 1 mm (approximately the width of the skin fold between the jaws when the clip was applied to the forearm skin of the human subject with 3–4 mm length of skin on each side). Next, we measured nociceptive sensations. The 25 subjects were instructed to use the Generalized Labeled Magnitude Scale (GLMS)[38,39] to make continuous ratings of the maximal perceived intensity of pain evoked during a one-minute pinch produced by the alligator clip applied to a fold of skin on the mid volar forearm. The GLMS was displayed on a computer screen and consisted of a vertical, thermometer-like scale with labels spaced quasi-logarithmically along its length from “No sensation”, at the bottom to “barely detectable”, “weak”, “moderate”, “strong”, “very strong”, and at the top, “strongest imaginable sensation of any kind”. The subject was told to rate continuously the maximal perceived intensity of pain regardless of its sensory quality by moving a cursor along the scale by means of a computer mouse. Subjects ratings were recorded continuously every 100 milliseconds of the 1-min pinch stimulation period, and evaluated and displayed as pain rating over time. The area under the curve (AUC) for the whole 1-min pinch stimulation for each subjects’ rating was calculated using GraphPad Prism 7. After the clip was removed, the subject was asked to rate the maximal perceived intensity of each of four aversive qualities of cutaneous sensation associated with the pain just experienced (viz., itch, pricking/stinging, burning and aching). Then they were asked to rate the intensity of any feeling of discomfort associated with this maximal sensation. The advantage of the GLMS is that it allows the perceived intensities of different cutaneous qualities to be compared on a common scale[40–42]. Before testing, the subjects were told that they might or might not experience one or more of these sensory qualities.

Statistics.

Statistical analyses were performed by using SigmaStat 3.5 and GraphPad Prism 7 software. All data sets were tested for normality for t-test, and if normality test failed, Mann-Whitney Rank Sum test was used. Results are expressed as mean ± s.e.m. or median ± quartile. $P < 0.05$ is considered as significant changes. For evaluation of ablation efficiency, and pinch- or blue light-evoked c-Fos induction, data were subjected to two-sided Student’s t-test. For pinch-evoked c-Fos in LHb and PBN regions, data was assessed by Two-way ANOVA

followed by post hoc Holm-Sidak's t-test. Chi-squared test (χ^2 test) was applied to determine the incidence of VPL innervation detected in thalamic sections, the incidence of licking evoked by the cold plate, and the incidence of recorded neurons showing activation by optogenetic stimulation. Behavior data was analyzed by using two-sided Student's t-test, Mann-Whitney Rank Sum test or Two-way ANOVA followed by post hoc Bonferroni's t-test. Human psychophysical data was analyzed with two-sided Student's t-test or Mann-Whitney Rank Sum test. The continuous pain ratings over time were analyzed by Two-way repeated measures ANOVA (gender × time).

Data availability.

All relevant data are available from the authors and included with the manuscript.

Extended Data

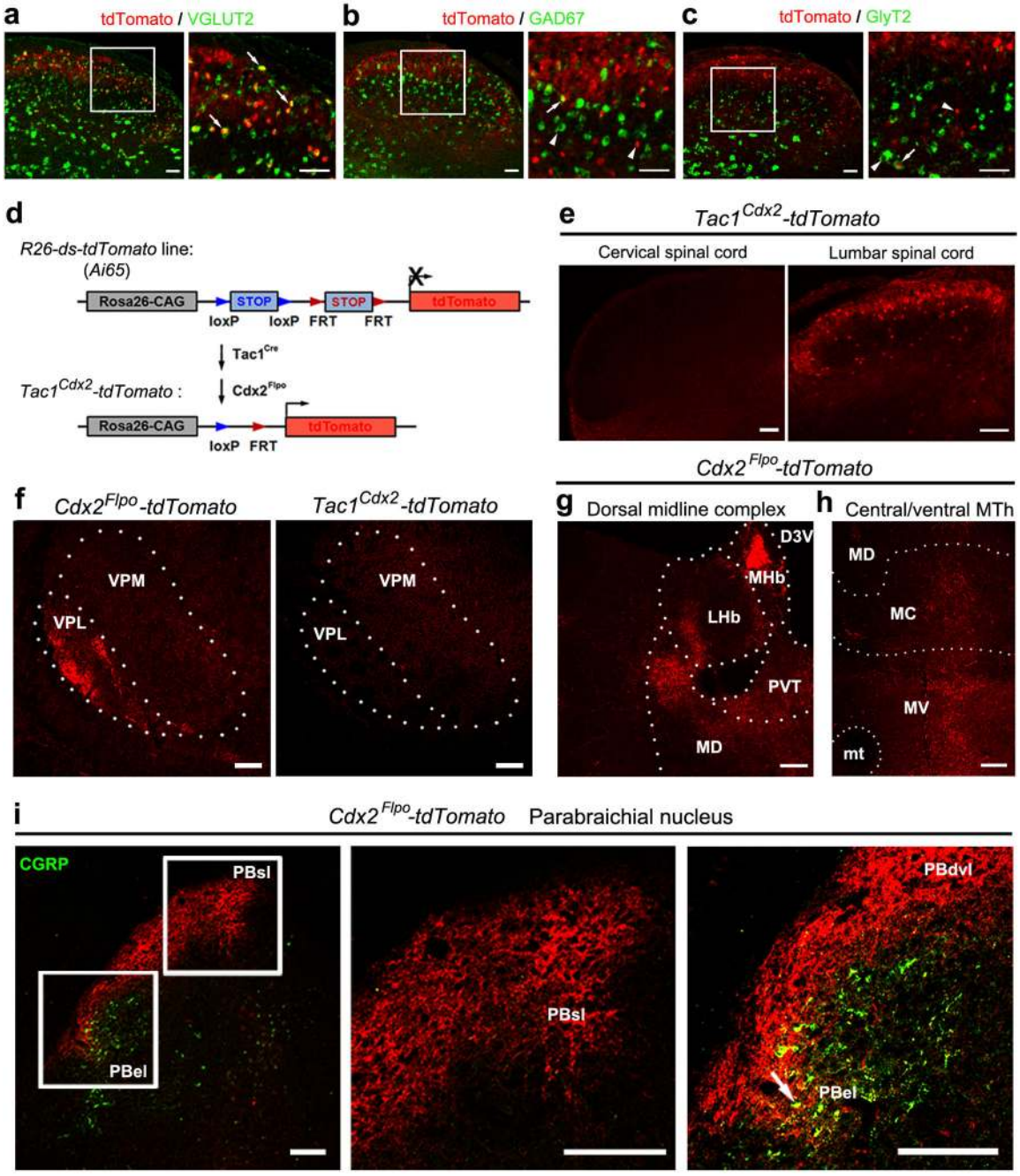

Extended Data Fig. 1. Neurotransmitter phenotypes and central projection by spinal Tac1^{Cre+} neurons.

a-c, Lumbar spinal sections from P30 *Tac1^{Cre}-tdTomato* mice (n = 3), in which spinal neurons with developmental expression of Tac1^{Cre} were labeled by tdTomato expression, showing double staining of tdTomato signals (red) and the mRNA of the excitatory neuronal marker VGLUT2 (**a**, green), or inhibitory neuronal markers GAD67 (**b**, green) and GlyT2 (**c**, green) detected by *in situ* hybridization[13]. Right panels represent higher magnification of

the boxed areas. Arrows show co-localization, and arrowheads show singular expression. Quantification of neurotransmitter phenotypes of spinal $Tac1^{Cre}$-tdTomato^{+} neurons: 91.2 ± 0.7% are VGLUT2^{+} excitatory neurons, 6.1 ± 1.1% are GAD67^{+} GABAergic inhibitory neurons, and 4.5 ± 0.9% are GlyT2^{+} glycinergic inhibitory neurons. data were presented as S.E.M. **d**, Intersectional genetic strategy for driving tdTomato expression in spinal $Tac1^{Cdx2}$ neurons defined by co-expression of $Tac1^{Cre}$ and $Cdx2^{Flpo}$. It had been reported previously that $Cdx2^{Flpo}$ drives reporter expression from the cervical spinal cord all the way to the most caudal spinal cord[6]. By crossing *Tac1*^{Cre} mice and *Cdx2*^{Flpo} mice with intersectional *Ai65* reporter mice, only spinal $Tac1^{Cre+}$ neurons co-expressed Flpo drove tdTomato expression, referred to as *Tac1*^{Cdx2}*-tdTomato* mice. **e**, Representative sections through the spinal cord of *Tac1*^{Cdx2}*-tdTomato* mice (n = 3), showing tdTomato^{+} neurons are not detected at the most rostral cervical levels or in the brain (data not shown), but are detected at the lumbar levels. **f**, Representative coronal sections (25 μm thick, prepared by cryostat, in comparison with Fig. 1c, which was 100 μm thick, prepared by vibratome) through the ventral lateral thalamus of *Cdx2*^{Flpo}*-tdTomato* mice (left, n = 3) and *Tac1*^{Cdx2}*-tdTomato* mice (right, n= 3). *Cdx2*^{Flpo}*-tdTomato* mice were generated by crossing *Cdx2*^{Flpo} mice with Flpo-dependent *ROSA26*$^{FSF\text{-}tdTomato}$ reporter mice. Among 25 μm thick VPL sections from *Tac1*^{Cdx2}*-tdTomato* mice, only 12% (3/26) showed sparse tdTomato signals, while 100% (26/26) of sections from *Cdx2*^{Flpo}*-tdTomato* mice showed robust tdTomato signals (CHI-test, $\chi^{2}_{.95,(1)} = 41.241$, $P < 0.001$). It should be noted that due to restriction of $Cdx2^{Flpo}$ to the spinal cord, no tdTomato signals were detected in the VPM of *Cdx2*^{Flpo}*-tdTomato* mice, since VPM is innervated by neurons located in the trigeminal nuclei or dorsal column nuclei that were not labeled by $Cdx2^{Flpo}$. **g-h**, Representative coronal sections (100 μm thick) through the thalamus of P30 *Cdx2*^{Flpo}*-tdTomato* mice (n = 2) at the level of Bregma −1.70 mm, showing the whole spinal ascending fibers in the medial thalamic complex. **i**, Representative coronal sections (25 μm) of parabrachial nuclei (PBN) from P30 *Cdx2*^{Flpo}*-tdTomato* mice (n = 2), showing tdTomato (red) and CGRP immunostaining (green). $Cdx2^{Flpo}$-tdTomato^{+} fibers send collateral terminals to CGRP^{+} PBel regions as indicated by the arrow, besides projection to PBel and PBdvl. D3V, third ventricular, dorsal division; LHb, lateral habenular nucleus; MC, mediocentral thalamic nucleus; MD, mediodorsal thalamic nucleus; MHb, medial habenular nucleus; mt, mammillothalamic tract; MTh, the medial thalamic nuclei that include MD, MC and MV; MV, medioventral thalamic nucleus; PBdvl, dorsal and ventral subnuclei of parabrachial nucleus; PBel, external lateral parabrachial nucles; PBsl, superior lateral parabrachial nucleus; PVT, paraventricular thalamic nucleus; LHb, lateral habenular nucleus; MTh, medial thalamic nucleus; PVT, paraventricular thalamic nucleus; VPL, ventral posterolateral thalamic nucleus; VPM, ventral posteromedial thalamic nucleus. Scale bars: 50 μm in **a-c**; 100 μm in **e-i**.

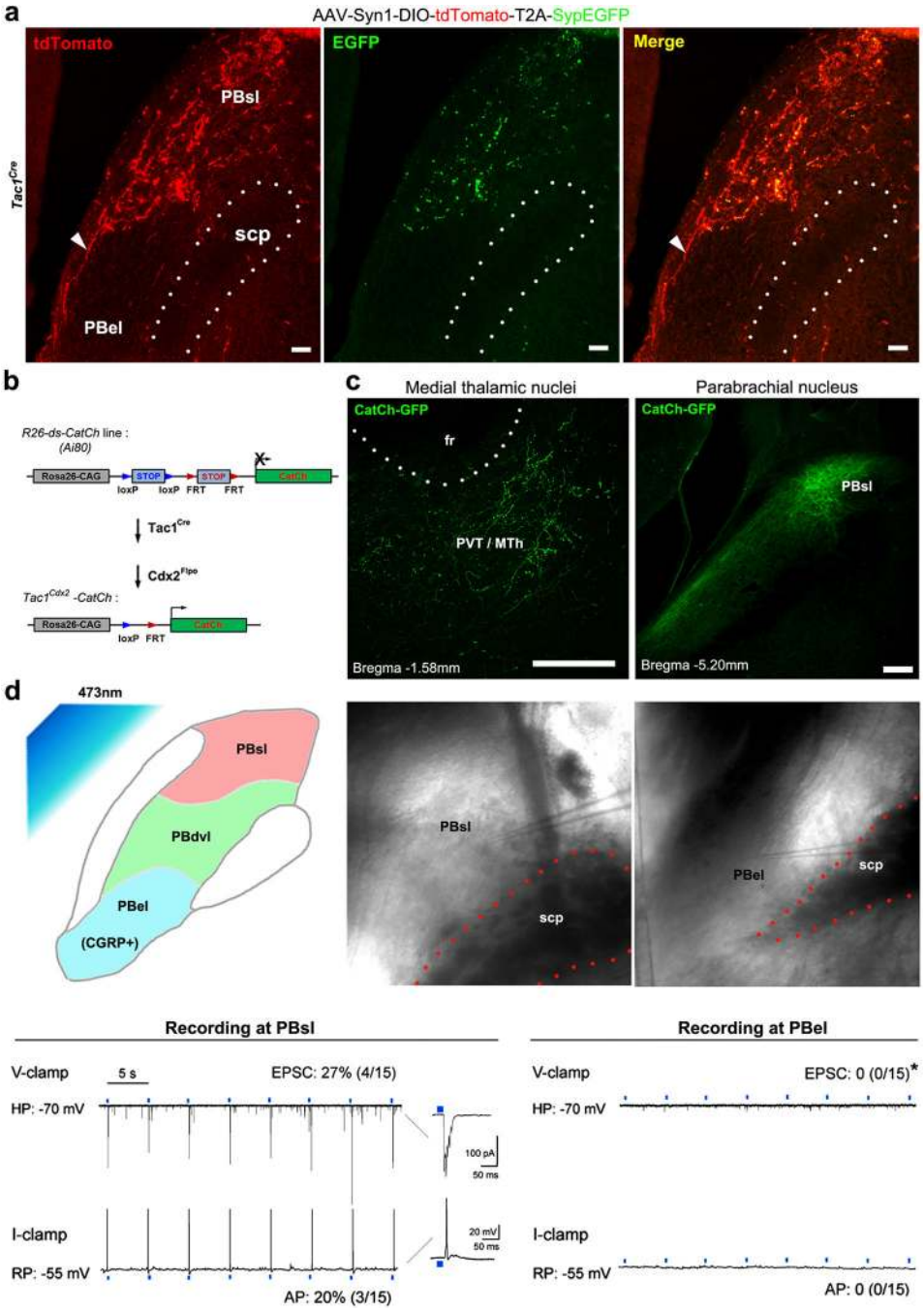

Extended Data Fig. 2. Functional connections of *Tac1*^{Cre}-derived neurons to neurons in PBsl.

a, Representative images showing the distribution of presynaptic reporter (the synaptophysin-EGFP fusion protein)[12] in the dorsal portion of lateral PBN including PBsl (**a**, middle, green), but not in the more ventral PBel, following intraspinal injection of the AAV-Syn1-DIO-tdTomato-T2A-SynEGFP virus at the lumbar level of adult *Tac1*^{Cre} mice (n = 2). The Tac1^{Cre+} axons are visualized by tdTomato signals (red). Arrowhead indicates the potential axons passing through ventral lateral PBN without making synapses. **b**, Intersectional genetic strategy for driving the expression of the calcium translocating

channelrhodopsin (CatCh, an L132C mutant channelrhodopsin with enhanced Ca^{2+} permeability and fused with GFP)[43] in spinal $Tac1^{Cdx2}$ neurons defined by co-expression of $Tac1^{Cre}$ and $Cdx2^{Flpo}$. This was achieved by crossing the intersectional CatCh mice (*Ai80*) with *Tac1*^{Cre} and *Cdx2*^{Flpo}, with the resulting triple heterozygous mice referred to as *Tac1*^{Cdx2}*-CatCh* mice. Triple heterozygous *Tac1*^{Cdx2}*-GFP* mice were used as control, which are generated by crossing *Tac1*^{Cre} and *Cdx2*^{Flpo} mice with intersectional GFP reporter mice *RC:: FrePe*. **c**, The ascending $Tac1^{Cdx2}$-CatCh-GFP^{+} terminals (observed from 3 mice) are detected in the medial thalamic region (left panel), including the paraventricular nucleus (PVT) and the medial thalamic nuclei (MTh). Right panel shows the GFP signals in the superior lateral parabrachial nucleus (PBsl), although the fluorescent signals of CatCh-GFP fusion protein detected by immunostaining are not as robust as by the direct visualization of tdTomato signals observed in *Tac1*^{Cdx2}*-tdTomato* mice shown in Figure 1. Scale bars: 100 μm. **d**, Upper, schematic diagram of optogenetic activation of $Tac1^{Cdx2}$-$CatCh^{+}$ terminals in the PBN area via 473 nm blue light, and recording sites for neurons in the PBsl or PBel nucleus of the same brain slices. Lower, voltage clamp (V-clamp) was used to record the evoked excitatory postsynaptic currents (EPSC), with holding membrane potential ("HP") at −70 mV. Current clamp was used to record action potential ("AP") firing. RP: resting membrane potential. Representative recording traces show that neurons in PBsl but not in PBel responded to the blue light stimulation (0.2 Hz, 20 ms, numbers of neurons with responses: PBsl, 4/15; PBel, 0/15; CHI-test, $\chi^2_{.95,(1)} = 4.615$, $P = 0.032$; *Tac1*^{Cdx2}*-CatCh* mice, n = 2).

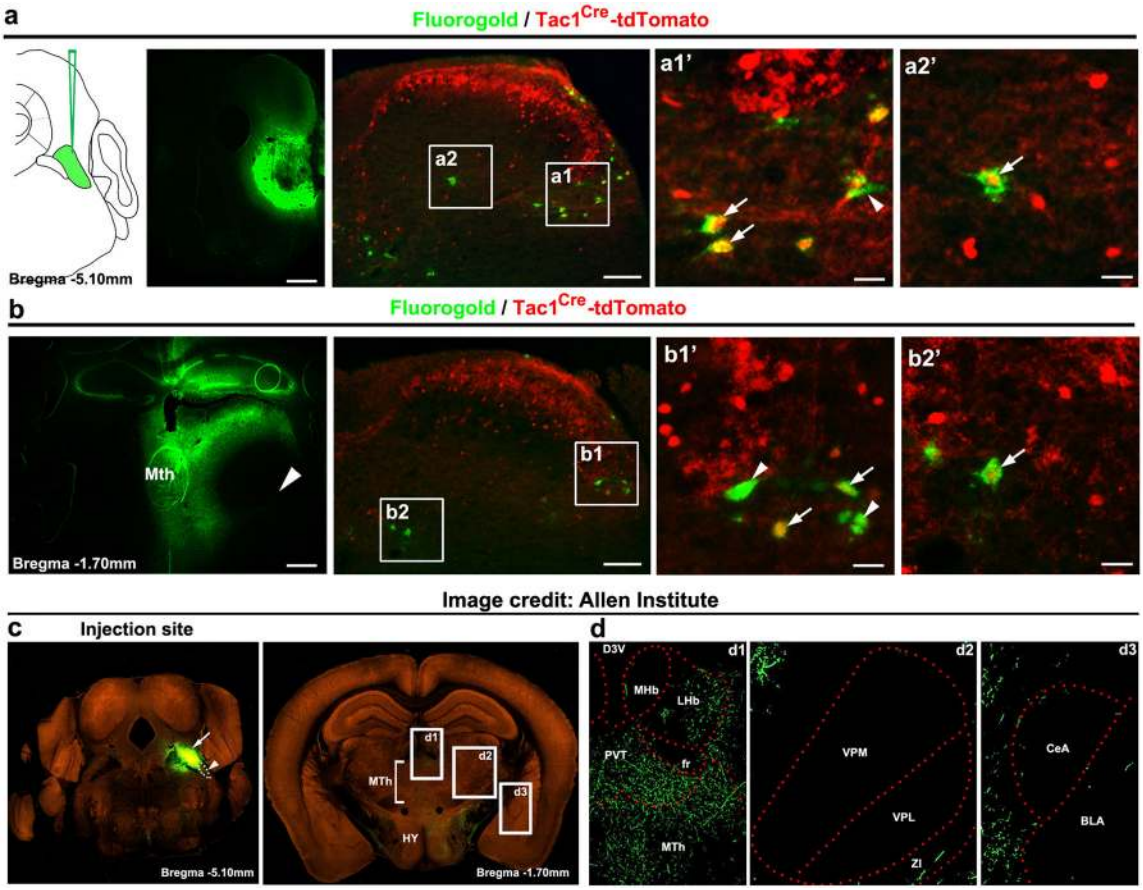

Extended Data Fig. 3. Retrograde labeling of spinal *Tac1*^{Cre}-derived projection neurons from parabrachial and medial thalamic nuclei and anterograde tracing from the dorsal part of lateral parabrachial nuclei (PBN).

a, Fluorogold retrograde labeling from the PBN of *Tac1*^{Cre}*-tdTomato* mice (n = 3). Left, the injection site. Middle and right, a representative transverse section of the dorsal horn showing Fluorogold^{+} retrograde labeled cells (green) and tdTomato^{+} *Tac1* lineage neurons (red). Arrows indicate colocalization in the lateral spinal nucleus (a1) and deep laminae (a2). Arrowhead indicates a tdTomato-negative retrograde labeled neuron, showing that *Tac1*^{Cre}-derived neurons represent a subset of spinoparabrachial projection neurons (n = 3, 27.2 ± 0.7%). **b,** Fluorogold retrograde labeling from the medial thalamic nuclei (MTh, n = 3 mice). Left, the injection site. Large arrowhead indicates that fluorogold injection didn't leak to the lateral VPM/VPL complex. Middle and right, a representative transverse section of the dorsal horn, showing Fluorogold^{+} retrograde labeled cells (green) and tdTomato^{+} *Tac1* lineage neurons (red). Arrows indicate colocalization in the lateral spinal nucleus (b1) and deep laminae (b2). Small arrowheads indicate tdTomato-negative retrograde labeled neurons, indicating that *Tac1*^{Cre}-derived neurons again represent a subset of spinothalamic projection neurons (n = 3 mice, 16.3 ± 3.8%). **c,** Anterograde tracing from dorsal lateral PBN (including superior lateral and dorsolateral subdivisions, PBsl and PBdvl, respectively). Image credit: Allen Institute. Left, the coronal plane (Bregma −5.10 mm) showing the injection site in parabrachial nuclei. Arrow indicates tracer injection confined to PBsl plus PBdvl. The white dot circle (arrowhead) indicates the external lateral PBN (PBel) that

contains none or little injected tracer. Right, the projection of PBsl-PBdvl neurons to thalamic and hypothalamic regions (Bregma −1.70 mm). Boxes d1, d2 and d3 highlight projections or lack of projections to the medial thalamic nuclei, the ventral lateral thalamic nuclei and the amygdaloid nuclei shown in **d,** respectively. HY, hypothalamic nuclei; MTh, medial thalamic nuclei. **d,** Dense innervations were observed in MTh (b1), the lateral habenular nucleus (b1, LHb), and the paraventricular nucleus of thalamus (b1, PVT). No innervations were observed in the medial or lateral parts of the ventral posterolateral nuclei (b2, VPM and VPL), or the central and basal lateral parts of amygdala (b3, CeA and BLA). The lack of innervations to CeA, which is innervated by $CGRP^+$ neurons in PBel[8], provided further indication that tracer injection to the PBsl-PBdvl region did not diffuse to the PBel region. The full set of tracing images is available at the Allen Mouse Brain Connectivity Atlas[12]: http://connectivity.brain-map.org/projection/experiment/siv/127469566?imageId=127469776&imageType=TWO_PHOTON,SEGMENTATION&initImage=TWO_PHOTON&x=18728&y=17591&z=3. The injection site picture is acquired and modified from image 104 of 140; the thalamic projection picture is acquired and modified from image 71 of 140.

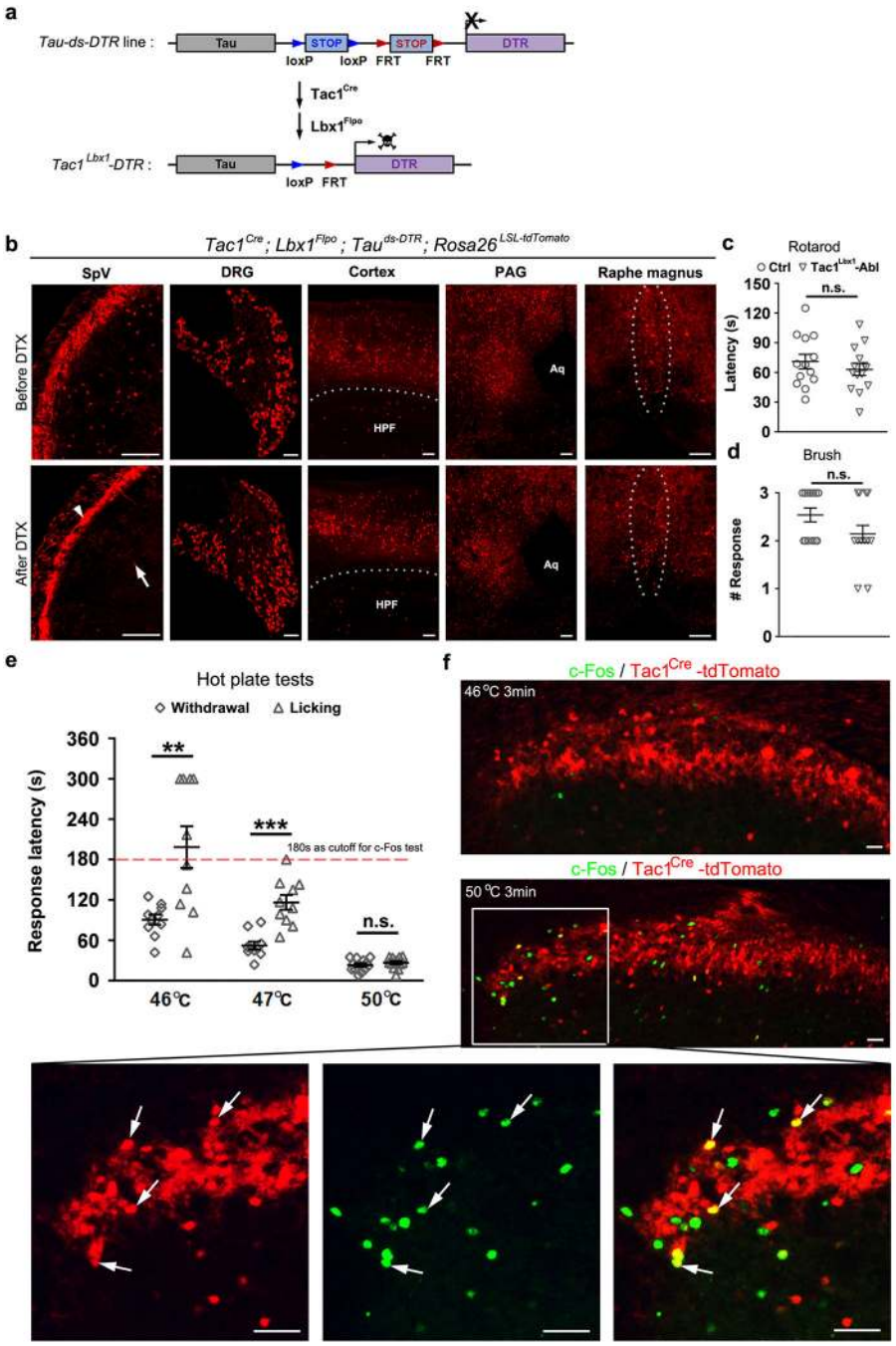

Extended Data Fig. 4. Additional anatomical and behavioral characterizations of Tac1^{Lbx1} neuron-ablated mice, as well as temporal segregation of withdrawal versus licking responses evoked by noxious heat and their correlation with c-Fos induction in Tac1^{Cre}-tdTomato^{+} neurons.

a, Intersectional genetic strategy for driving DTR expression selectively in dorsal spinal cord Tac1^{Lbx1} neurons defined by co-expression of Tac1^{Cre} and Lbx1^{Flpo}. DTR is driven from the pan-neural promoter *Tau*, and its expression needs removal of two STOP cassettes by Cre and Flpo DNA recombinases. Lbx1^{Flpo} expression is confined to the dorsal hindbrain and dorsal spinal cord within the nervous system[6,13]. **b**, Representative images showing a

marked loss of tdTomato$^+$ cells in the hindbrain spinal trigeminal nucleus (SpV) after DTX injections (n = 3 mice). Arrow in SpV indicates one of few remaining cells and arrowhead indicates processes derived from Tac1^{Cre}-tdTomato$^+$ trigeminal primary afferents that were preserved. Tac1^{Cre}-tdTomato$^+$ neurons are preserved in dorsal root ganglia (DRG) and trigeminal ganglia (not shown), as well as in various brain regions such as the cortex, hippocampus formation (HPF), periaqueductal gray nuclei (PAG) or raphe magnus. Aq, aqueduct. **c**, No detected difference in falling latencies from the rotarod between control littermates and Tac1^{Lbx1} neuron-ablated mice ("Tac1^{Lbx1}-Abl") (control, n = 13; Tac1^{Lbx1}-Abl, n = 14; two-sided t-test, $P = 0.403$). **d**, No detected difference in response rates to gentle hind paw brushing (out of three tries for each mouse) between control and Tac1^{Lbx1}-Abl groups (control, n = 13; Tac1^{Lbx1}-Abl, n = 14; two-sided Mann-Whitney Rank Sum test, $P = 0.121$). **e**, wild type mice showed distinct latencies of lifting/flinching versus licking in response to hot plate stimulation set at 46–47 °C, but no difference at 50 °C (46 °C, n = 10, two-sided paired t-test, $P = 0.006$; 47 °C, n = 10, two-sided paired t-test, $P < 0.001$; 50 °C, n = 12, two-sided paired t-test, $P = 0.379$). In 46 °C hot plate test, licking responses were rarely observed within the first 3 min. **f**, Representative immunostaining of c-Fos in superficial dorsal horn of *Tac1^{Cre}-tdTomato* mice 2 hours after 3-min exposure at the 46 °C or 50 °C hot plate (n = 3 for each condition). Only 50 °C could induce significant amount of c-Fos expression. Lower panels represent the boxed area. Arrows indicate colocalization of c-Fos (green) with Tac1^{Cre}-tdTomato$^+$ cells (red). Scale bars: 100 μm in **b**, 25 μm in **f**. Data was presented as mean ± s.e.m. in **c**, **e**; and median ± quartile in **d**.

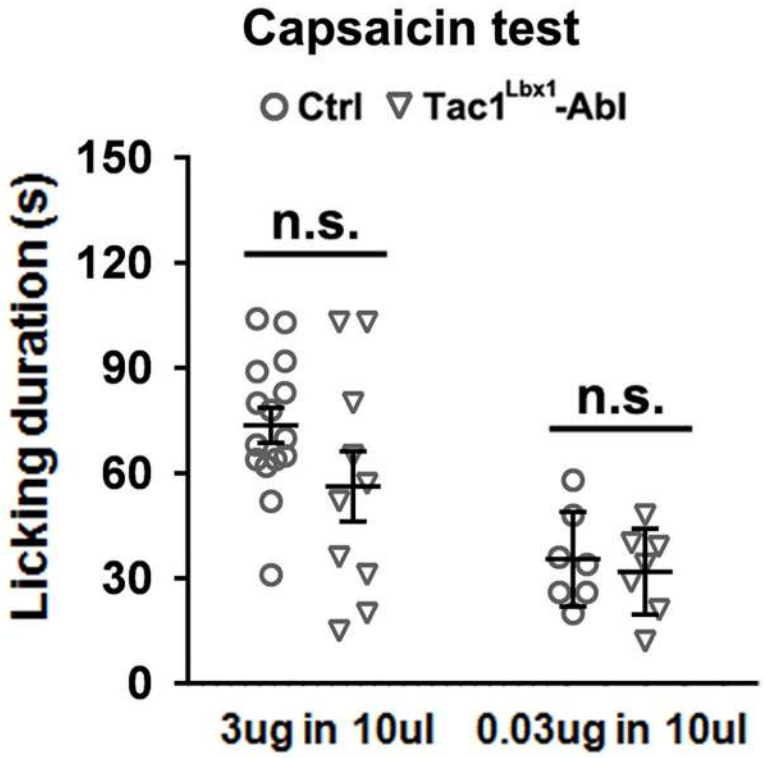

Extended Data Fig. 5. Tac1^{Lbx1} neuron-ablated mice still produced licking responses to intraplantar capsaicin injection.

No difference in licking evoked by 10 μl solution containing 3 μg (left) or 0.03 μg (right) capsaicin (3 μg-test: control, n = 15; $Tac1^{Lbx1}$-Abl, n = 10, two-sided t-test, $t_{(23)} = 1.714$, $P = 0.143$; 0.03 μg-test: control, n = 7; $Tac1^{Lbx1}$-Abl, n = 7, two-sided t-test, $t_{(12)} = 0.519$, $P = 0.613$), suggesting the existence of $Tac1^{Lbx1}$ neuron-independent pain pathways. This preservation of capsaicin-evoked licking is drastically different from a complete loss of licking evoked by mustard oil (MO) and other noxious stimuli (Fig. 3). Licking responses evoked by mustard oil at low concentration (≤0.75%) is dependent on TRPA1[44], and TRPA1 is expressed in a subset of $TRPV1^+$ neurons[45]. As such, MO-responsive neurons only represent a subset of capsaicin-responsive neurons[46,47]. In other words, there are capsaicin-sensitive, MO-insensitive, neurons that could in principle mediate $Tac1^{Lbx1}$ neuron-independent licking evoked by capsaicin. Data shown as mean ± s.e.m..

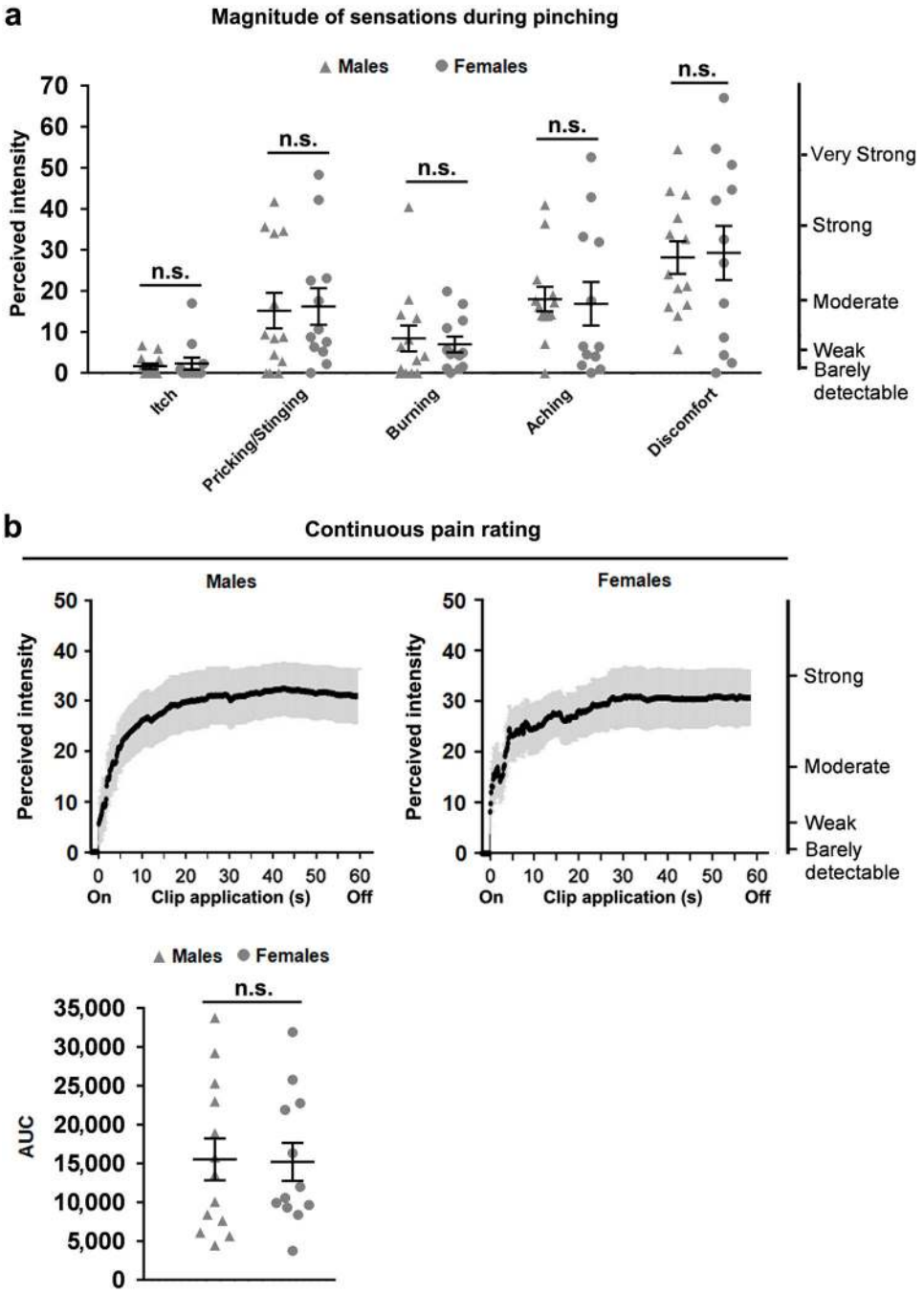

Extended Data Fig. 6. Skin pinch evoked sustained pain in humans.

During application of the alligator clip, both female and male subjects were instructed to rate continuously the perceived intensity of pain regardless of its quality. After the clip was removed, each subject was asked to rate, in similar fashion, the maximal perceived intensity of each of four aversive qualities of cutaneous sensation associated with the pain just experienced. The four sensory qualities were itch, pricking/stinging, burning and aching. Then subjects were asked to rate the discomfort associated with this maximal sensation. The common scale at the right side indicates the intensity of each sensation (see Methods for

detail). **a**, no differences between male (n = 13) and female (n = 12) human subjects in rating the magnitude of the indicated sensory qualities (two-sided Mann Whitney Rank Sum test, itch: U = 75.0, $P = 0.874$; pricking/stinging: U = 69.5, $P = 0.663$; burning: U =71.0, $P = 0.723$; Aching: U = 62.5, $P = 0.414$; two-sided t-test, discomfort: $t_{(23)} = -0.150$, $P = 0.882$; data shown as mean ± s.e.m.). **b**, no differences in the continuous pain rating between males (n = 13) and females (n = 12) (upper, continuous pain rating at different time points during the 1-min pinch period were subjected to Two-way ANOVA analyses with repeated measures, and no significant difference was detected between genders, $F_{(1, 23)} = 0.008$, $P = 0.929$; lower, the areas under the entire curve, "AUC", again did not show a difference between genders, two-sided t-test, $t_{(23)} = 0.089$, $P = 0.929$, data shown as mean ± s.e.m.). This lack of detectable gender differences with the current sample sizes is consistent with previous studies showing that gender differences for experimentally evoked pain are not easy to detect in humans[48,49].

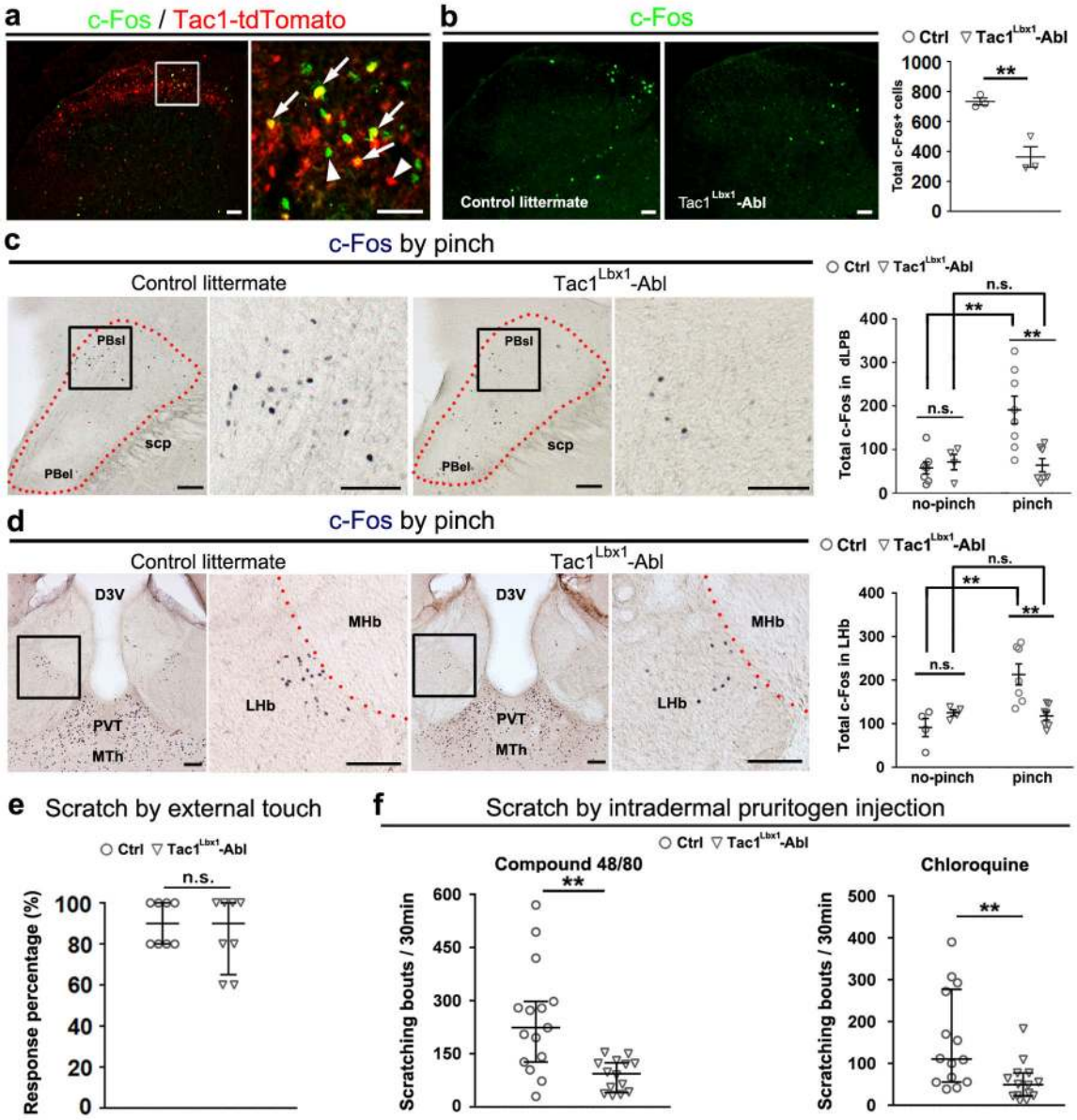

Extended Data Fig. 7. Loss of pinch-induced c-Fos expression in the dorsal horn, the PBsl nucleus, and the lateral habenula, and attenuated pruritogen-induced scratching in Tac1^{Lbx1} neuron-ablated mice.

a, Representative lumbar spinal cord sections of P60 *Tac1^{Cre}-tdTomato* mice (n = 4) after hindpaw pinch stimulation. 41.7 ± 8.0% neurons with pinch-induced c-Fos co-expressed tdTomato. Arrows indicate co-localization and arrowheads indicate singular expression. **b**, Reduced c-Fos in lumbar dorsal horn of Tac1^{Lbx1}-Abl mice (n = 3 mice for each group, two-sided t-test, $P = 0.007$). **c**, Representative images showing pinch-induced c-Fos on coronal sections through the lateral parabrachial nuclei (PBN). Note in wild type littermates, pinch-induced c-Fos was enriched in the superior lateral PBN (PBsl), rarely in external lateral PBN (PBel). Right panel shows quantification of c-Fos^{+} cells between Bregma −5.24 and −4.96 mm, with and without pinching (no-pinch group: control littermates, n = 7; Tac1^{Lbx1}-Abl, n = 4; pinch group: control littermates, n = 8; Tac1^{Lbx1}-Abl, n = 7). Two-way ANOVA

indicates significant interactions between genotypes and pinch stimulation ($F_{(1,22)} = 8.555$, $P = 0.008$); post hoc comparison (Holm-Sidak method) shows comparable basal level c-Fos expression (no-pinch groups, $P = 0.72$), an increase in control littermates within the PBsl ($P = 0.004$), and the loss of this increase in Tac1^{Lbx1}-Abl mice ($P = 0.006$). **d**, Representative coronal sections through the dorsal midline thalamic complex, showing bilateral c-Fos induction by pinch, which is in consistent with previous electrophysiological studies[50,51]. Right panel shows the counting of pinch-induced c-Fos$^+$ cells in an LHb region adjacent to the MHb from Bregma −1.46 to −2.06 mm (no-pinch groups: control littermates, n = 4; Tac1^{Lbx1}-Abl, n =4; pinch groups: control littermates, n = 7; Tac1^{Lbx1}-Abl, n = 7). Two-way ANOVA indicates significant interactions between genotypes and pinch stimulation ($F_{(1,18)} = 11.08$, $P = 0.004$); post hoc comparison (Holm-Sidak method) shows comparable basal level c-Fos expression (no-pinch groups, $P = 0.289$), significant increase in control littermates' LHb ($P = 0.008$), and loss of this increase in Tac1^{Lbx1}-Abl mice ($P = 0.003$). Due to high background c-Fos expression in the paraventricular thalamic nucleus (PVT) and medial thalamic nuclei (MTh), we cannot determine pinch-evoked neuronal activation in these nuclei. **e**, No difference in scratching response rates evoked by light von Frey filament stimulation (control: n = 8; Tac1^{Lbx1}-Abl: n = 8; two-sided Mann-Whitney Rank Sum test, $P = 0.721$). **f**, Reduced scratching bouts induced by intradermal pruritogen injection (compound 48/80: control, n = 15; Tac1^{Lbx1}-Abl, n = 14; two-sided Mann-Whitney Rank Sum test, $P = 0.002$; chloroquine: control, n = 14; Tac1^{Lbx1}-Abl, n = 14; two-sided Mann-Whitney Rank Sum test, $P = 0.005$). "Ctrl": control littermates. n.s.: $P > 0.05$. **b-d**, data shown as mean ± s.e.m.; **e**, **f**, data shown as mean ± quartile. Scale bars: 50 μm in **a** and **b**, 100 μm in **c** and **d**.

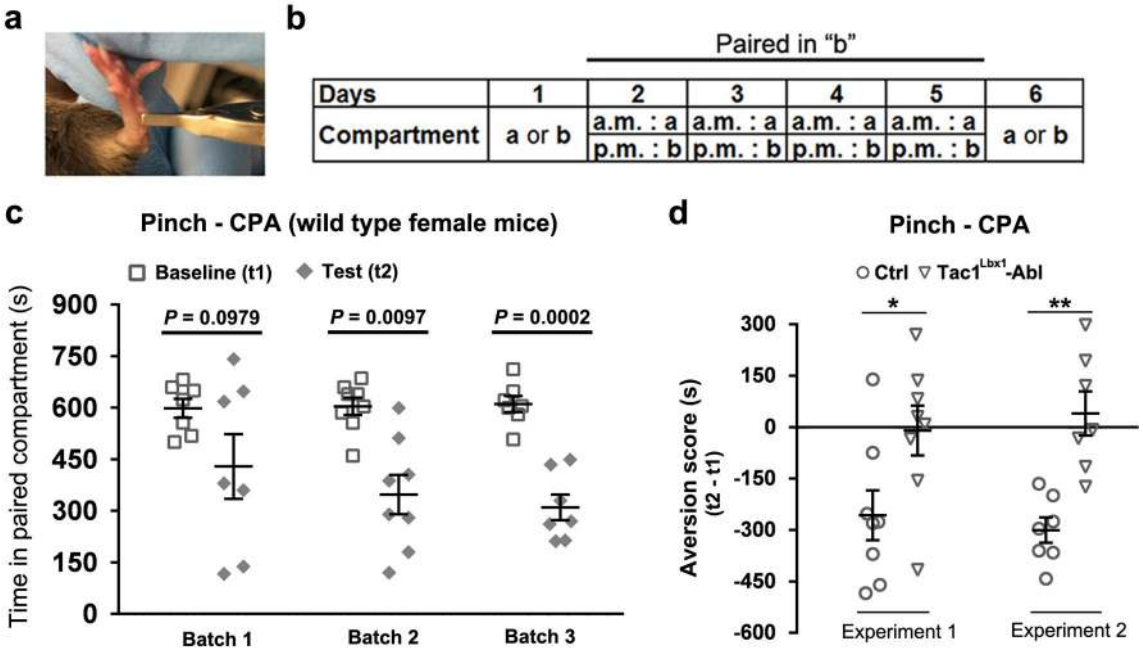

Extended Data Fig. 8. Loss of pinch-induced CPA in Tac1^{Lbx1}-neuron ablated female mice.
a, A pinched mouse hindpaw. The alligator clip was applied to the ventral skin surface between the footpad and the heel. **b**, The experimental paradigm for pinch-evoked CPA test

(for details, see Methods). **c**, Hindpaw skin pinch, but not sham handling (grabbing without pinching, data not shown), induced CPA in wild type females. CPA is measured by the change of time staying in the paired chamber before (baseline, t1) and after (test, t2) pinch-evoked conditioning. In 3-independent batches of wild type control littermates, two-sided t-test showed that the second and third batches, but not the first batch, displayed significant reduction of t2 in comparison with t1 (two-sided t-test: batch 1, n = 7, p = 0.0979; batch 2, n = 8, P = 0.0097; batch 3, n = 7, P = 0.0002). Two-Way ANOVA analyses of these three batches indicated pinch-evoked avoidance to the paired chamber ($F_{(1,19)} = 36.514$, $P < 0.001$), without showing batch effects ($F_{(2,19)} = 0.547$, $P = 0.587$) and interactions ($F_{(2,19)} = 0.885$, $P = 0.429$), suggesting that pinch can induce CPA in wild type females. **d**, $Tac1^{Lbx1}$ neuron-ablated female mice showed a loss of pinch-induced CPA (control littermates and $Tac1^{Lbx1}$-Abl mice, n = 8 for experiment 1, t-test, $*P = 0.031$; n = 7 for experiment 2, t-test, $**P = 0.001$), as male mice did (Fig. 3).

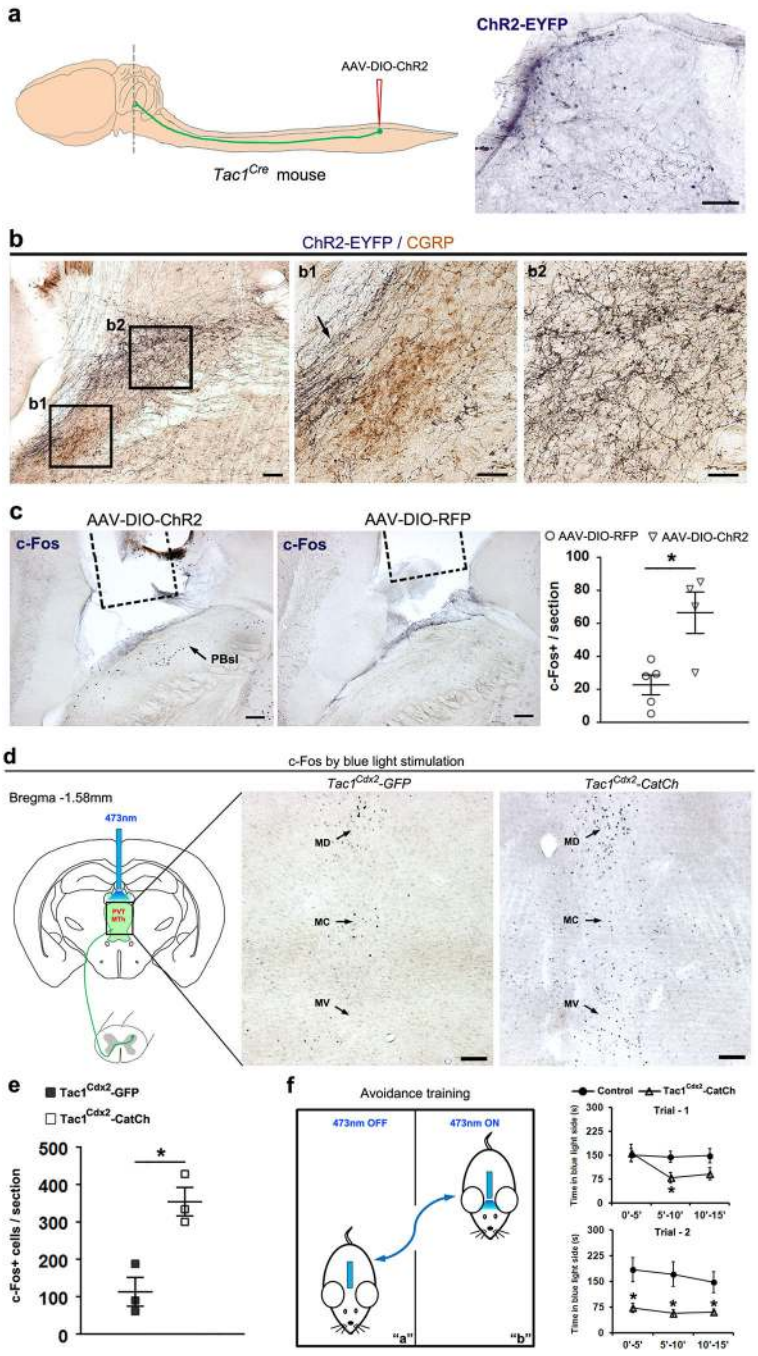

Extended Data Fig. 9. Optogenetic activation of Tac1^{Cre}-derived ascending terminals around the parabrachial nucleus (PBN, a-c) or medial thalamus (d-f).

a-c, Viral infection in lumbar spinal cord Tac1^{Cre+} neurons and subsequent optogenetic activation of the central terminals in the PBN area. **a**, The AAV-DIO-ChR2 virus, which drove the expression of the fusion ChR2-EYFP protein in a Cre-dependent manner, was injected into the lumbar dorsal horn of *Tac1^{Cre}* mouse, and the ascending ChR2-EYFP^{+} terminals around the PBN (dash line) were visualized by a GFP antibody. These mice are referred to as Tac1^{Cre}-ChR2 mice. Right, immunostaining shows ChR2-EYFP fusion protein

expression in the lumbar spinal cord. **b**, Representative images showing double-color immunostaining, revealing the ascending projections to the PBN at Bregma −5.02 mm. Tac1^{Cre}-ChR2-EYFP^{+} terminals (dark blue) were co-stained with CGRP (brown). Note that Tac1^{Cre}-ChR2-EYFP^{+} fibers pass through a region (**b1**, arrow) lateral to the CGRP^{+} external lateral PBN (**b1**, PBel, brown), and terminated densely in the superior lateral PBN (**b2**, PBsl). **c**, Representative images showing Blue light stimulation-induced c-Fos expression in PBsl of Tac1^{Cre}-ChR2 mice, with much fewer c-Fos^{+} neurons following blue light stimulation in control Tac1^{Cre}-RFP mice, in which viral injection drove the expression of RFP but not ChR2 (ChR2 mice, n = 4; RFP control mice, n = 5; two-sided t-test, $P = 0.012$). Dashed lines indicate the location of the implanted optic fiber in the region right above the PBN. **d-f**, Optogenetic experiments for spinal Tac1 neurons projected to medial thalamic nuclei (MD, MC and MV). **d,e**, Generation of the intersectional Tac1^{Cdx2}-CatCh^{+} mice was described in Extended Data Figure 2b. The optic fiber was implanted above the medial thalamic complex (left scheme). Neuronal activation by blue light stimulation was indicated by the increase of c-Fos^{+} cells in *Tac1^{Cdx2}-CatCh* mice in comparison with *Tac1^{Cdx2}-GFP* mice, as shown by representative images and quantitative analyses (Tac1^{Cdx2}-CatCh: n = 3; Tac1^{Cdx2}-GFP: n = 3; two-sided t-test, $P = 0.011$). **f**, The *Tac1^{Cdx2}-CatCh* mice showed progressive avoidance to the blue light-paired chamber during two 15 min-training trials conducted at two consecutive days (see Methods for detail). Two-way ANOVA plus post hoc Bonferroni's t-test showed a progressive avoidance to the paired chamber (*Tac1^{Cdx2}-CatCh* mice, n = 10; *Tac1^{Cdx2}-GFP* control mice, n = 11; trial 1, significant interaction, $F_{(2,38)} = 5.067$, $P = 0.011$; trial 2, significant genotype effect, $F_{(1,19)} = 6.825$, $P = 0.017$, no interaction, $F_{(2,38)} = 0.73$, $P = 0.489$).

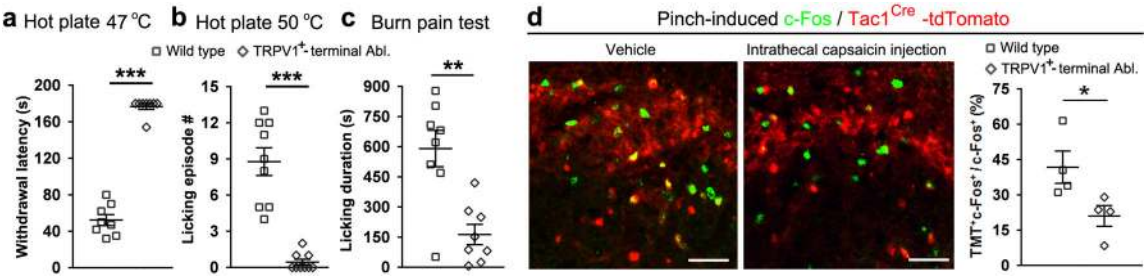

Extended Data Fig. 10. Ablation of TRPV1^{+} central terminals led to impaired responses to noxious heat or skin burn injury, as well as a reduction of pinch-induced c-Fos expression in dorsal horn Tac1^{Cre}-tdTomato^{+} neurons.

a, TRPV1^{+} central terminal-ablated mice showed a dramatic increase in the withdrawal latency evoked by the 47°C hot plate stimulation, with cut off time set at 3 min (vehicle injection versus intrathecal capsaicin injection groups, n = 8 for each group, two-sided Mann-Whitney Rank Sum test, ***$P < 0.001$). This is stark contrast to subtle, insignificant changes seen in Tac1^{Lbx1} neuron-ablated mice (Fig. 2e). **b**, Loss of licking behavior evoked by the 50 °C hot plate stimulation (vehicle injection versus intrathecal capsaicin injection groups, n = 9 for each group; licking episodes within one min, two-sided Mann-Whitney Rank Sum test, ***$P < 0.001$). **c**, TRPV1^{+} central terminal-ablated mice also displayed a dramatic reduction in licking evoked by hindpaw burn injury (n = 8 for each group, licking duration within 30 min after skin burn injury, two-sided t-test, $P = 0.001$). **d**, Representative

immunostaining images and quantitative analyses showing pinch-evoked c-Fos expression (green) in the dorsal horn of *Tac1*^{Cre}*-tdTomato* mice, with or without chemical ablation of TRPV1^{+} central terminals (n = 4 for each group). Note a reduction of pinch-induced c-Fos expression in Tac1^{Cre}-tdTomato^{+} cells after ablation of TRPV1^{+} central terminals (two-sided t-test, $P = 0.044$).

TRPV1^{+} nociceptors are necessary for both reflexes[20] (**a**), and licking (**b** and **c**) evoked by noxious heat. Earlier studies showed that those DRG neurons with highest TRPV1 expression (TRPV1^{highest}), representing about 10% of TRPV1^{+} nociceptors[52], respond to moderate warm-hot stimulation[53]. Like Mrgprd^{+} nociceptors, these TRPV1^{highest} neurons innervate exclusively the skin epidermis[53] and their development is dependent on the same transcription factor Runx1[52,54]. We therefore speculate that these TRPV1^{highest} neurons may involve with first-line reflexes evoked by noxious heat, raising the possibility that there are different subsets of TRPV1^{+} nociceptors associated with reflexes versus sustained pain evoked by noxious heat. Future experiments are needed to test this hypothesis.

Supplementary Material

Refer to Web version on PubMed Central for supplementary material.

Acknowledgement

We thank Z.J. Huang, M.J. Zylka, M. Hoon, S.M. Dymecki, and the Allen Brain Institute/the Jackson Laboratory for genetically modified mice, Drs. A.I. Basbaum, A.V. Apkarian and C.J. Woolf for constructive discussions, and Y. Liu and Z. He for viral reagents. All data are contained in the main text and supplementary materials. The anterograde tracing data is from Allen Brain Atlas website (http://connectivity.brain-map.org/). The work was supported by NIH grants to Q.M. (R01 DE018025) and to Q.M. and M.G. (R01 NS086372), the Wellcome Trust grant to Q.M. (200183/Z/15/Z), and the Research Fellowship (326726541) from the German Research Foundation (DFG) to N.M.M..

References and Notes

1. Mark VH, Ervin FR & Yakovlev PI Stereotactic thalamotomy III. The verification of anatomical lesion sites in the human thalamus. Archives of neurology 8, 528–538 (1963).
2. Young RF et al. Gamma Knife thalamotomy for the treatment of persistent pain. Stereotact Funct Neurosurg 64 Suppl 1, 172–181 (1995). [PubMed: 8584825]
3. Price DD Central neural mechanisms that interrelate sensory and affective dimensions of pain. Mol Interv 2, 392–403, 339, doi:10.1124/mi.2.6.392 (2002). [PubMed: 14993415]
4. Gutierrez-Mecinas M et al. Preprotachykinin A is expressed by a distinct population of excitatory neurons in the mouse superficial spinal dorsal horn including cells that respond to noxious and pruritic stimuli. Pain 158, 440–456, doi:10.1097/j.pain.0000000000000778 (2017). [PubMed: 27902570]
5. Todd AJ Neuronal circuitry for pain processing in the dorsal horn. Nat Rev Neurosci. 11, 823–836 (2010). [PubMed: 21068766]
6. Bourane S et al. Identification of a spinal circuit for light touch and fine motor control. Cell 160, 503–515 (2015). [PubMed: 25635458]
7. Head H & Holmes HJ Sensory disturbances from cerebral lesions. Brain 81, 102–154 (1911).
8. Han S, Soleiman MT, Soden ME, Zweifel LS & Palmiter RD Elucidating an Affective Pain Circuit that Creates a Threat Memory. Cell 162, 363–374, doi:10.1016/j.cell.2015.05.057 (2015). [PubMed: 26186190]
9. Rodriguez E et al. A cranio-facial-specific monosynaptic circuit enables hieghtened affective pain. Nature Neuroscience 20, 1734–1743 (doi:1710.1038/s41593-41017-40012-41591) (2017). [PubMed: 29184209]

10. Yahiro T, Kataoka N, Nakamura Y & Nakamura K The lateral parabrachial nucleus, but not the thalamus, mediates thermosensory pathways for behavioural thermoregulation. Sci Rep 7, 5031, doi:10.1038/s41598-017-05327-8 (2017). [PubMed: 28694517]
11. Mu D et al. A central neural circuit for itch sensation. Science 357, 695–699, doi:10.1126/science.aaf4918 (2017). [PubMed: 28818946]
12. Oh SW et al. A mesoscale connectome of the mouse brain. Nature 508, 207–214, doi:10.1038/nature13186 (2014). [PubMed: 24695228]
13. Duan B et al. Identification of spinal circuits transmitting and gating mechanical pain. Cell 159, 1417–1432, doi:10.1016/j.cell.2014.11.003 (2014). [PubMed: 25467445]
14. Bourane S et al. Gate control of mechanical itch by a subpopulation of spinal cord interneurons. Science 350, 550–554 (2015). [PubMed: 26516282]
15. Melzack R & Wall PD Pain mechanisms: a new theory. Science 150, 971–979 (1965). [PubMed: 5320816]
16. Duan B, Cheng L & Ma Q Spinal Circuits Transmitting Mechanical Pain and Itch. Neurosci Bull 34, 186–193, doi:10.1007/s12264-017-0136-z (2018). [PubMed: 28484964]
17. Arenas OM et al. Activation of planarian TRPA1 by reactive oxygen species reveals a conserved mechanism for animal nociception. Nat Neurosci 20, 1686–1693, doi:10.1038/s41593-017-0005-0 (2017). [PubMed: 29184198]
18. Vandewauw I et al. A TRP channel trio mediates acute noxious heat sensing. Nature 555, 662–666, doi:10.1038/nature26137 (2018). [PubMed: 29539642]
19. Ward L, Wright E & McMahon SB A comparison of the effects of noxious and innocuous counterstimuli on experimentally induced itch and pain. Pain 64, 129–138 (1996). [PubMed: 8867255]
20. Cavanaugh DJ et al. Distinct subsets of unmyelinated primary sensory fibers mediate behavioral responses to noxious thermal and mechanical stimuli. Proc Natl Acad Sci U S A. 106, 9075–9080 (2009). [PubMed: 19451647]
21. Zylka MJ, Rice FL & Anderson DJ Topographically distinct epidermal nociceptive circuits revealed by axonal tracers targeted to Mrgprd. Neuron. 2005 1 6;45(1):17–25 45, 17–25 (2005). [PubMed: 15629699]
22. Cavanaugh DJ et al. Restriction of transient receptor potential vanilloid-1 to the peptidergic subset of primary afferent neurons follows its developmental downregulation in nonpeptidergic neurons. J Neurosci. 31, 10119–10127 (2011). [PubMed: 21752988]
23. Malin S et al. TRPV1 and TRPA1 function and modulation are target tissue dependent. J Neurosci. 31, 31 (2011).
24. Cheng L et al. Identification of spinal circuits involved in touch-evoked dynamic mechanical pain. Nat Neurosci 20, 804–814, doi:10.1038/nn.4549 (2017). [PubMed: 28436981]
25. Adriaensen H, Gybels J, Handwerker HO & Van Hees J Nociceptor discharges and sensations due to prolonged noxious mechanical stimulation--a paradox. Hum Neurobiol 3, 53–58 (1984). [PubMed: 6330012]
26. Schmidt R, Schmelz M, Torebjork HE & Handwerker HO Mechano-insensitive nociceptors encode pain evoked by tonic pressure to human skin. Neuroscience 98, 793–800 (2000). [PubMed: 10891622]
27. Schmelz M, Schmid R, Handwerker HO & Torebjork HE Encoding of burning pain from capsaicin-treated human skin in two categories of unmyelinated nerve fibres. Brain 123 Pt 3, 560–571 (2000). [PubMed: 10686178]
28. Cobos EJ & Portillo-Salido E “Bedside-to-Bench” Behavioral Outcomes in Animal Models of Pain: Beyond the Evaluation of Reflexes. Curr Neuropharmacol. 11, 560–591 (2013). [PubMed: 24396334]
29. Borsook D, Hargreaves R, Bountra C & Porreca F Lost but making progress--Where will new analgesic drugs come from? Sci Transl Med 6, 249sr243, doi:10.1126/scitranslmed.3008320 (2014).
30. LeDoux JE & Pine DS Using Neuroscience to Help Understand Fear and Anxiety: A Two-System Framework. Am J Psychiatry 173, 1083–1093, doi:10.1176/appi.ajp.2016.16030353 (2016). [PubMed: 27609244]

31. Niederkofler V et al. Identification of Serotonergic Neuronal Modules that Affect Aggressive Behavior. Cell Rep 17, 1934–1949, doi:10.1016/j.celrep.2016.10.063 (2016). [PubMed: 27851959]
32. Britz O et al. A genetically defined asymmetry underlies the inhibitory control of flexor-extensor locomotor movements. Elife 4, doi:10.7554/eLife.04718 (2015).
33. Liu Y et al. VGLUT2-dependent glutamate release from peripheral nociceptors is required to sense pain and suppress itch. Neuron 68, 543–556 (2010). [PubMed: 21040853]
34. Lou S, Duan B, Vong L, Lowell BB & Ma Q Runx1 controls terminal morphology and mechanosensitivity of VGLUT3-expressing C-mechanoreceptors. J Neurosci. 33, 870–882 (2013). [PubMed: 23325226]
35. Knowlton WM, Bifolck-Fisher A, Bautista DM & McKemy DD TRPM8, but not TRPA1, is required for neural and behavioral responses to acute noxious cold temperatures and cold-mimetics in vivo. Pain 150, 340–350 (2010). [PubMed: 20542379]
36. Brenner DS, Golden JP & Gereau R. W. t. A novel behavioral assay for measuring cold sensation in mice. PLoS One 7, e39765, doi:10.1371/journal.pone.0039765 (2012). [PubMed: 22745825]
37. Pogorzala LA, Mishra SK & Hoon MA The cellular code for Mammalian thermosensation. J Neurosci. 33, 5533–5541 (2013). [PubMed: 23536068]
38. Green BG et al. Evaluating the 'Labeled Magnitude Scale' for measuring sensations of taste and smell. Chem Senses 21, 323–334 (1996). [PubMed: 8670711]
39. Bartoshuk LM et al. Valid across-group comparisons with labeled scales: the gLMS versus magnitude matching. Physiol Behav 82, 109–114, doi:10.1016/j.physbeh.2004.02.033 (2004). [PubMed: 15234598]
40. Green BG & Schoen KL Thermal and nociceptive sensations from menthol and their suppression by dynamic contact. Behav Brain Res 176, 284–291, doi:10.1016/j.bbr.2006.10.013 (2007). [PubMed: 17092576]
41. LaMotte RH, Shimada SG, Green BG & Zelterman D Pruritic and nociceptive sensations and dysesthesias from a spicule of cowhage. J Neurophysiol 101, 1430–1443, doi:10.1152/jn.91268.2008 (2009). [PubMed: 19144738]
42. Sikand P, Shimada SG, Green BG & LaMotte RH Sensory responses to injection and punctate application of capsaicin and histamine to the skin. Pain 152, 2485–2494 (2011). [PubMed: 21802851]
43. Kleinlogel S et al. Ultra light-sensitive and fast neuronal activation with the Ca(2)+-permeable channelrhodopsin CatCh. Nat Neurosci 14, 513–518, doi:10.1038/nn.2776 (2011). [PubMed: 21399632]
44. Kwan KY et al. TRPA1 contributes to cold, mechanical, and chemical nociception but is not essential for hair-cell transduction. Neuron 50, 277–289 (2006). [PubMed: 16630838]
45. Story GM et al. ANKTM1, a TRP-like channel expressed in nociceptive neurons, is activated by cold temperatures. Cell 112, 819–829 (2003). [PubMed: 12654248]
46. Bautista DM et al. TRPA1 mediates the inflammatory actions of environmental irritants and proalgesic agents. Cell 124, 1269–1282 (2006). [PubMed: 16564016]
47. Wang S et al. Phospholipase C and protein kinase A mediate bradykinin sensitization of TRPA1: a molecular mechanism of inflammatory pain. Brain 131, 1241–1251 (2008). [PubMed: 18356188]
48. Bartley EJ & Fillingim RB Sex differences in pain: a brief review of clinical and experimental findings. Br J Anaesth 111, 52–58, doi:10.1093/bja/aet127 (2013). [PubMed: 23794645]
49. Doehring A et al. Effect sizes in experimental pain produced by gender, genetic variants and sensitization procedures. PLoS One 6, e17724, doi:10.1371/journal.pone.0017724 (2011). [PubMed: 21423693]
50. Giesler GJ Jr., Yezierski RP, Gerhart KD & Willis WD Spinothalamic tract neurons that project to medial and/or lateral thalamic nuclei: evidence for a physiologically novel population of spinal cord neurons. J Neurophysiol 46, 1285–1308 (1981). [PubMed: 7320746]
51. Benabid AL & Jeaugey L Cells of the rat lateral habenula respond to high-threshold somatosensory inputs. Neurosci Lett 96, 289–294 (1989). [PubMed: 2717054]

52. Abdel Samad O et al. Characterization of two Runx1-dependent nociceptor differentiation programs necessary for inflammatory versus neuropathic pain. Mol Pain 6, 45 (2010). [PubMed: 20673362]

53. Kiasalari Z et al. Identification of perineal sensory neurons activated by innocuous heat. J Comp Neurol. 518, 137–162 (2010). [PubMed: 19937707]

54. Chen CL et al. Runx1 determines nociceptive sensory neuron phenotype and is required for thermal and neuropathic pain. Neuron 49, 365–377 (2006). [PubMed: 16446141]

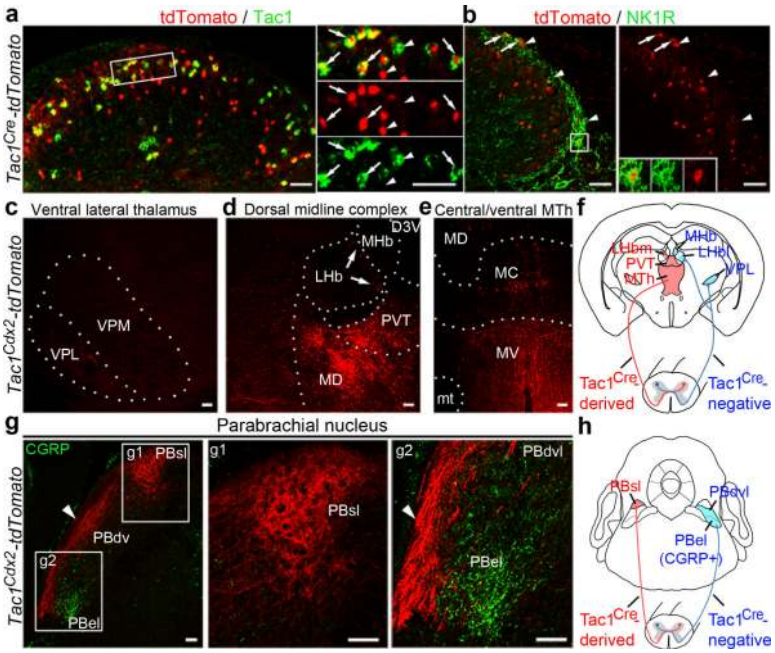

Fig. 1. Spinal Tac1 neurons project to medial thalamic and superior lateral parabrachial nuclei.

a, b, Representative sections from P30 (postnatal day 30) *Tac1*^{Cre}*-tdTomato* mice (n = 3), showing tdTomato (red) with Tac1 mRNA (green) or NK1R (green) in superficial dorsal spinal laminae. Arrows indicate co-localization and arrowheads indicate singular expression. Inset in (**b**) shows a NK1R^{+}/tdTomato^{+} cell. **c-e**, Representative coronal thalamic sections (100 μm, Bregma −1.70 mm) from P30 *Tac1*^{Cdx2}*-tdTomato* mice (n = 3). Arrows in (**d**) indicate the most medial part of LHb. **f**, Schematic summary of thalamic projections. **g**, Representative PBN sections from P30 *Tac1*^{Cdx2}*-tdTomato* mice (n = 3), showing tdTomato (red) and CGRP immunostaining (green). Note innervations in PBsl (**g1**). Arrowheads in (**g2**) indicate fibers passing through the area lateral to PBdvl and CGRP^{+} PBel. **h**, Schematic summary of parabrachial projections. D3V, third ventricular, dorsal division; LHb, lateral habenular nucleus; LHbm and LHbl: the medial and lateral parts of LHb, respectively; MC, MD and MV, mediocentral, mediodorsal and medioventral thalamic nuclei, respectively; MHb, medial habenular nucleus; mt, mammillothalamic tract; MTh, the medial thalamic nuclei including MD, MC and MV; PBdvl, PBel and PBsl: the dorsoventral, external and superior lateral PBN, respectivley; PVT, paraventricular thalamic nucleus; scp, superior cerebellar peduncle; VPL, ventral posterolateral thalamic nucleus; VPM, ventral posteromedial thalamic nuclei. Scale bars: 50 μm.

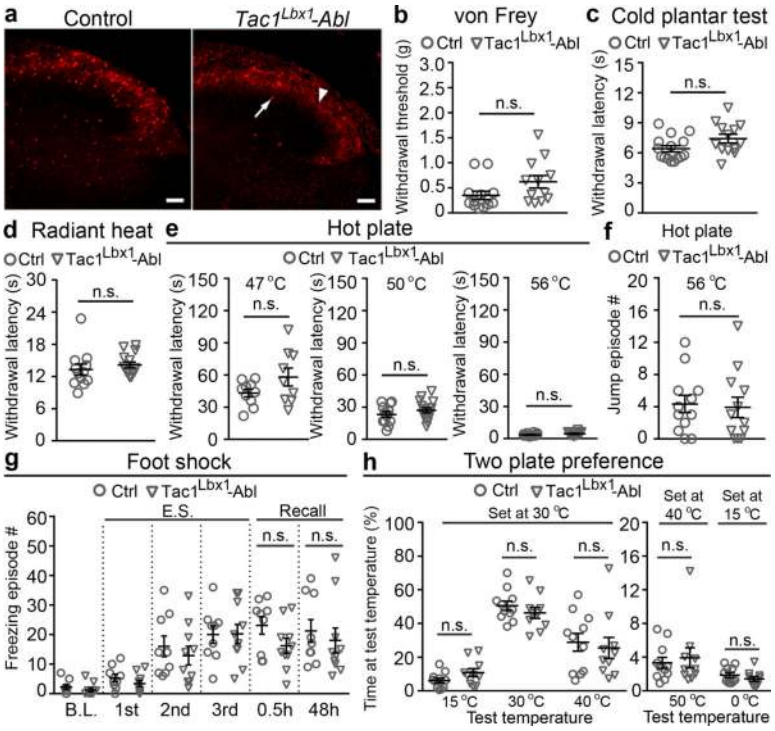

Fig. 2. Tac1 ^{Lbx1} neurons are dispensable for reflexive-defensive reactions.

a, Tac1^{Lbx1} neuron-ablated (Tac1^{Lbx1}-Abl) mice showed loss of spinal Tac1^{Cre}-tdTomato^{+} neurons (control, n = 4, 97 ± 7; Tac1^{Lbx1}-Abl, n = 4, 11 ± 3; $P < 0.001$). Arrow indicates a remaining cell and arrowhead indicates processes from un-ablated primary afferents. Scale bars: 100 μm. **b-e**, Reflexive response tests. No significant (n.s.) differences in withdrawal responses to von Frey filament (**b**, $P = 0.09$), cold (**c**, $P = 0.07$), radiant heat (**d**, $P = 0.44$), or hot plate (**e**, $P = 0.11$, 0.28, and 0.12 for 47 °C, 50 °C, and 56 °C, respectively) stimulus (control: n=13, 15, and 12 for **b-d**, respectively, for **e**, n=10, 12, and 14 for 47 °C, 50 °C, and 56 °C, respectively; Tac1^{Lbx1}-Abl: n=12, 13, and 14 for **b-d**, respectively, for **e**, n=9, 15, and 12 for 47 °C, 50 °C, and 56 °C, respectively). **f**, Comparable jumping evoked by 56 °C hot plate (control and Tac1^{Lbx1}-Abl, n = 12, $P = 0.80$). **g**, Foot shock test. Control (n = 9) and Tac1^{Lbx1}-Abl (n =10) groups showed no difference in freezing episodes by three repeated electrical stimulations ("E.S.") (Two-way ANOWA, $P = 0.86$), and no difference during recall phases (two-sided t-test: 0.5h, $P = 0.10$; 48h, p =0.58; mean ± s.e.m). **h**, Two-plate preference tests. No difference in time spending at the test versus the set temperatures (control: n=11; Tac1^{Lbx1}-Abl: n=10; $P = 0.10$, 0.33, 0.69, 0.67, and 0.28 for test temperatures at 15 °C, 30 °C, 40 °C, 50 °C, and 0 °C, respectively). **a-f**, **h**, two-sided t-test. Data shwon as mean ± s.e.m.

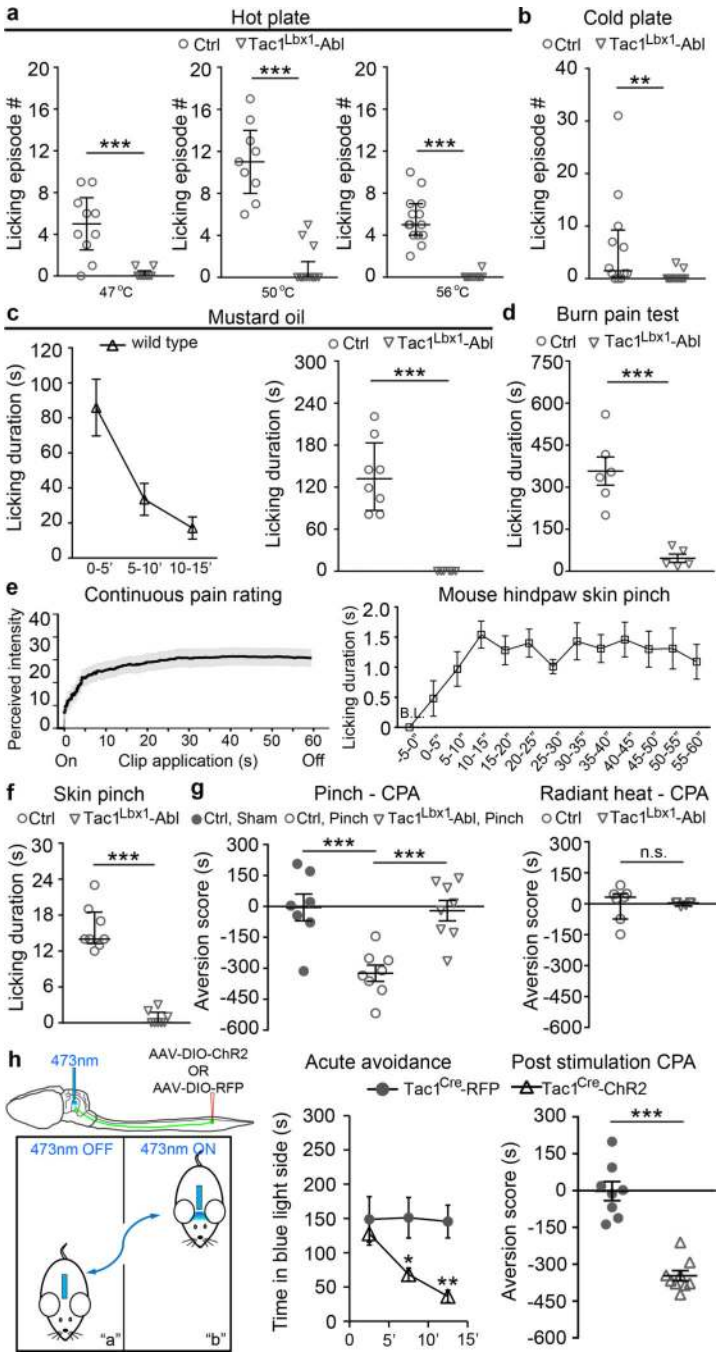

Fig. 3. Tac1 ^{Lbx1} neurons are required for noxious stimuli-evoked licking and conditioned place aversion (CPA), and their activation drove CPA.

a-b, Tac1^{Lbx1} neuron-ablated (Tac1^{Lbx1}-Abl) mice lost licking evoked by hot plate (**a**, control: 47 °C, n=10; 50 °C, n=12; 56 °C, n=14; Tac1^{Lbx1}-Abl: 47 °C, n=9; 50 °C, n=15; 56 °C, n=12, $P < 0.001$) or cold plate (**b**, control, n=12; Tac1^{Lbx1}-Abl, n=15, $P = 0.002$; χ^2 test for incidence of mice with licking, control, 9/12; Tac1^{Lbx1}-Abl, 2/15; $\chi^2_{.95,(1)} = 10.5$, $P = 0.001$). **c**, mustard oil injection. Left, licking time course in wild type mice (n = 8). Right, loss of licking in Tac1^{Lbx1}-Abl mice (control, n=8; Tac1^{Lbx1}-Abl, n=6, $P < 0.001$). **d**,

Reduced licking evoked by hindpaw burn injury (control, n=6; Tac1^{Lbx1}-Abl, n=5; two-sided t-test, $P = 0.001$; mean ± s.e.m). **e**, Skin pinching tests. Left, continuous pain ratings during a one-min period (human subjects, n=25). Right, licking time course in wild type mice (n=10), counted every 5 seconds within a one-min period. **f**, Loss of pinch-evoked licking in Tac1^{Lbx1}-Abl mice (control and Tac1^{Lbx1}-Abl, n = 8; $P < 0.001$). **g**, Hindpaw skin pinch induced CPA in control male mice (sham handling group, n=7; pinched group, n=8; two-sided t-test, $P < 0.001$; mean ± s.e.m), and CPA loss in Tac1^{Lbx1}-Abl mice (pinched control and Tac1^{Lbx1}-Abl, n=8; two-sided t-test, $P < 0.001$; mean ± s.e.m). Radiant heat did not generate CPA (control and Tac1^{Lbx1}-Abl, n=6, two-sided Mann-Whitney Rank Sum test, $P = 0.234$, mean ± quartile). **h**, Left, intraspinal AAV injection and PBN implantation of the optic fiber in adult *Tac1^{cre}* mice. Blue light was on (30 Hz, 20 ms pulse width, 10 mW) whenever a mouse entered compartment “b”. Middle and right, optogenetic activation of terminals in PBN (control RFP mice, n=8; ChR2 mice, n=9) induced both acute avoidance (middle, Two-way ANOVA followed by two-sided post hoc Bonferroni’s t-test, $*P = 0.012$, $**P = 0.002$) and CPA 24 hours later (right, two-sided t-test, $P < 0.001$; mean ± s.e.m). **a-c**, **f**, two-sided Mann-Whitney Rank Sum test, data shown as mean ± quartile.

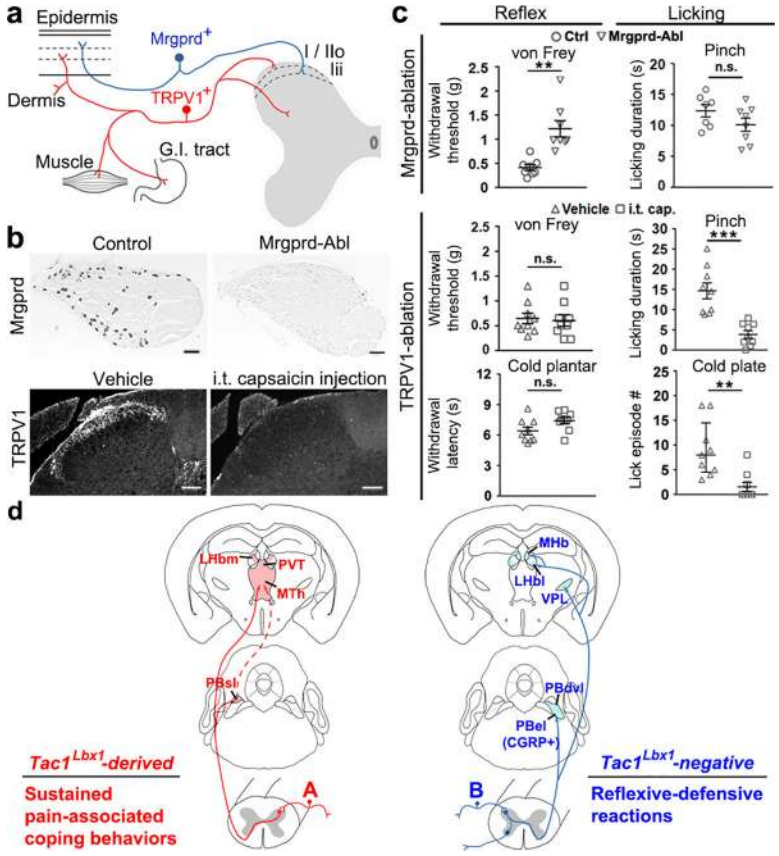

Fig. 4. TRPV1$^+$, but not Mrgprd$^+$ neurons are required for noxious stimuli-evoked licking.

a, Mrgprd$^+$ and TRPV1$^+$ neurons innervate distinct peripheral targets and spinal laminae. G.I.: gastrointestinal. **b**, Upper, representative *in situ* hybridization on DRG sections from three pairs of mice, indicating ablation of Mrgprd$^+$ neurons; lower, representative immunostaining images from 3 pairs of mice, showing ablation of TRPV1$^+$ terminals in superficial spinal lamianes following intrathecal (i.t) capsaicin injection. Scale bars: 100 μm. **c**, Upper, reduced reflexive responses to von Frey filaments in Mrgprd neuron-ablated (Mrgprd-Abl) mice (control and Abl, n=8, two-sided t-test, $P = 0.002$), without affecting pinch-evoked licking (control, n=7; Abl, n=8, two-sided t-test, $P = 0.150$). Lower, TRPV1$^+$ terminal-ablated (TRPV1-Abl) mice (vehicle and capsaicin groups, n=9) showed reduced licking by pinch (two-sided t-test, $P < 0.001$) or cold plate (Mann-Whitney Rank Sum test for licking episode, $P = 0.002$; χ^2 test for incidence of mice with licking, control, 9/9; TRPV1-Abl, 3/9; $\chi^2_{.95,(1)} = 9$, $P = 0.003$), without affecting withdrawal responses (two-sided t-test; von Frey, $P = 0.797$; cold plantar test, $P = 0.060$). **d**, Summary of two pathways required to drive sustained pain-associated coping behaviors versus reflexive-defensive reactions to external threats. "A" and "B" represents separate primary sensory neurons. "A" includes TRPV1$^+$ neurons required for licking evoked by pinch, noxious cold/heat, and skin burn injury, and "B" includes Mrgprd$^+$ neurons for reflexes evoked by von Frey filaments (for additional discussion, see Extended Data Fig.10). Data was presented as mean ± s.e.m., except cold plate test (median ± quartile).